Nonabelian Plasma Instabilities

Michael Strickland

Frankfurt Institute for Advanced Studies

XXXVI International Symposium on Multiparticle Dynamics

6 September 2006

Motivation

- We would like to have a first principles derivation of the mechanisms and time scales necessary for the isotropization and equilibration of a quark-gluon plasma.
- In addition to equilibration via 2-2 elastic scattering (super slow) one needs to include inelastic processes, e.g. bremsstrahlung 2-3 (and 3-2) processes, and the effect of *background fields*.
- In equilibrium the background fields (soft modes) only serve to screen the interaction (Debye screening). However, in a non-equilibrium setting the background field can have non-trivial dynamics and can have a big effect on the particles' motion.
- Consider, for example, a spatially homogeneous plasma which has been initialized such that it has a "temperature" anisotropy.
- In such an anisotropic plasmas new collective modes corresponding to *electro-/chromodynamic instabilities* appear.

Why anisotropic distribution functions?

Because of the natural expansion of the system the gluon distribution functions created during relativistic heavy ion collisions are *generically* locally anisotropic in momentum space.

$$
\begin{aligned}
<p_T> \quad &\sim \quad Q_s \qquad \text{(nuclear saturation scale)} \\
<p_L> \quad &\sim \quad 1/\tau \qquad \text{(free streaming)}
\end{aligned}
$$

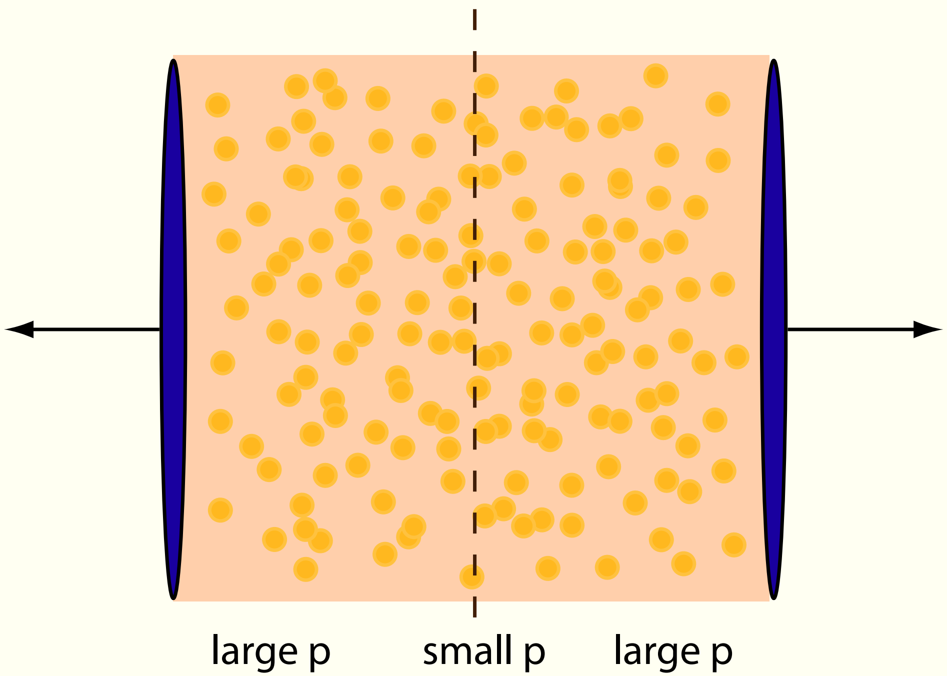

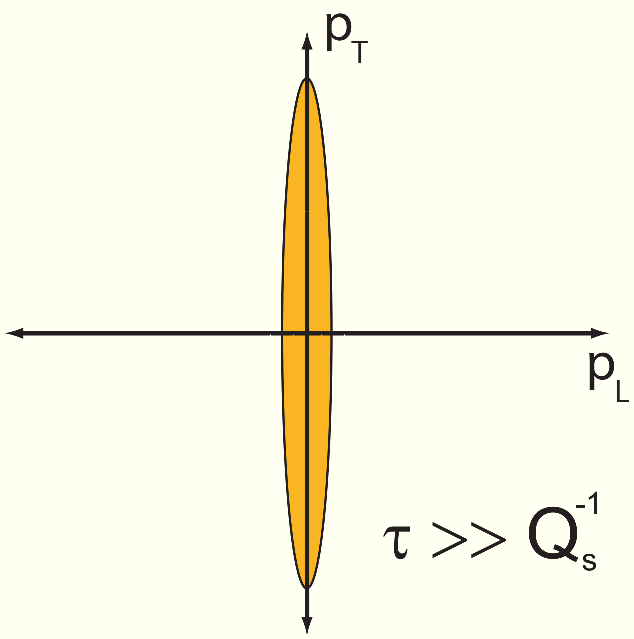

Momentum Space Anisotropy Time Dependence

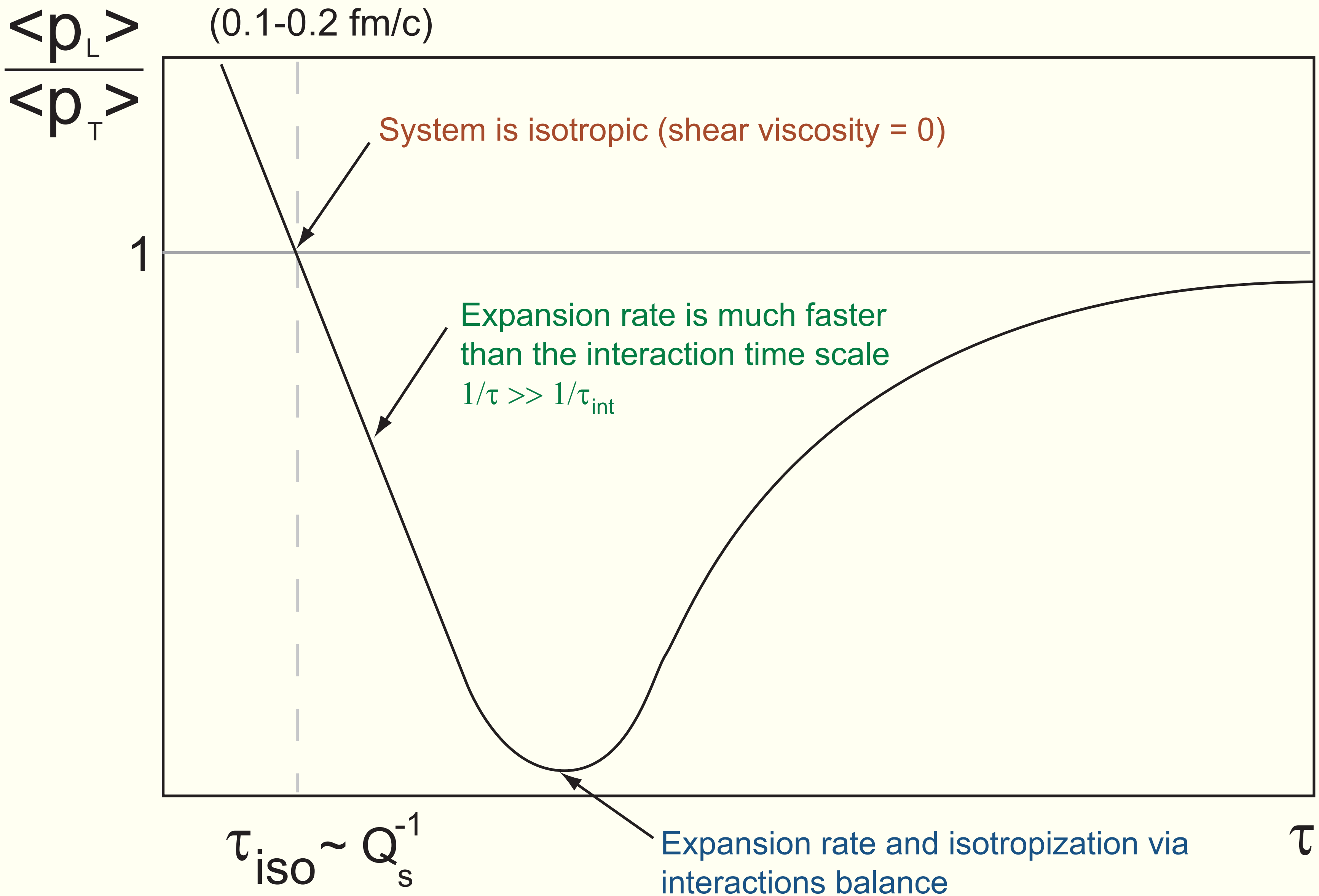

Current Filamentation

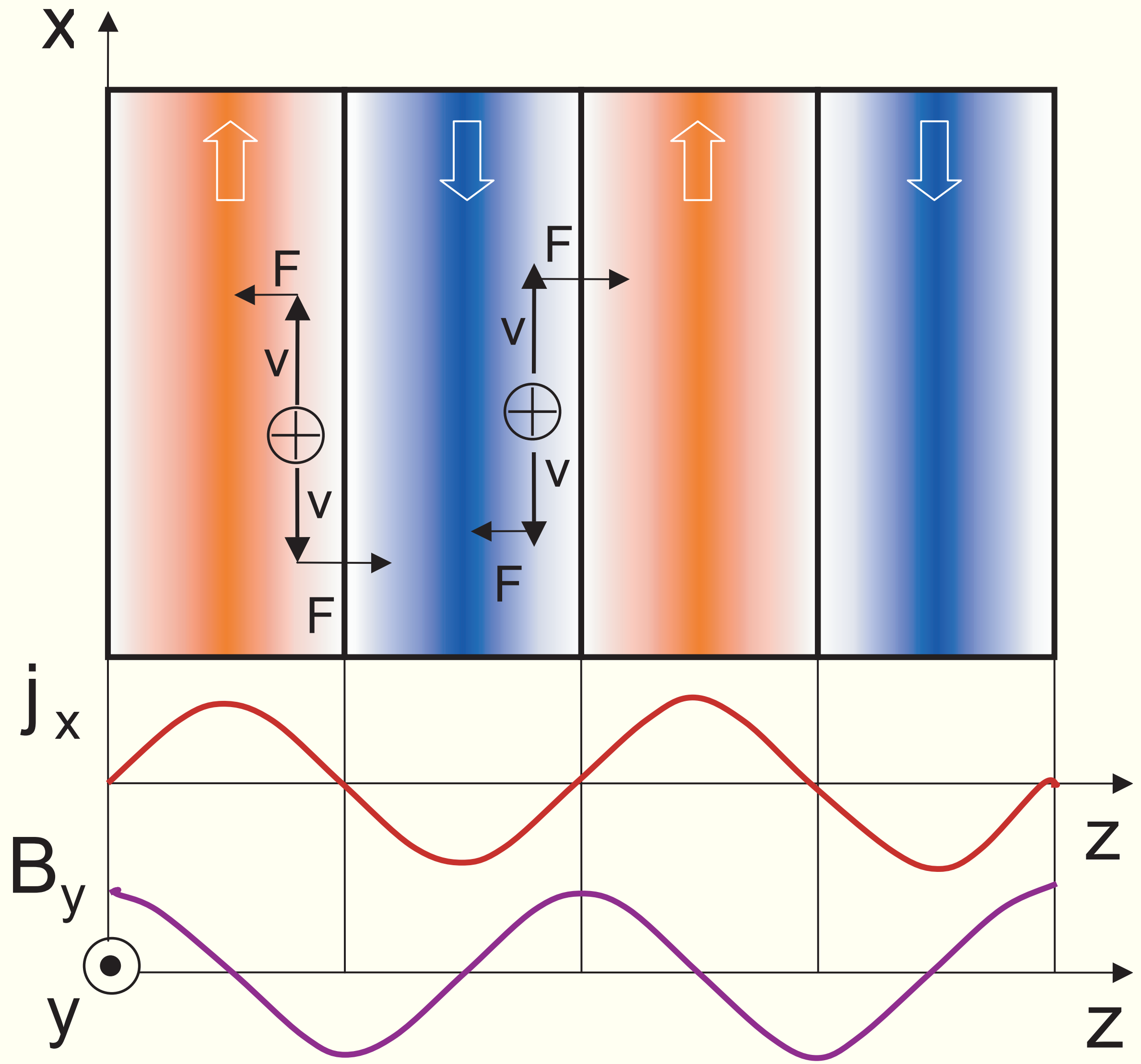

Figure adapted from S. Mrówczyński, hep-ph/0511052.

Abelian Plasma – The Weibel Instability

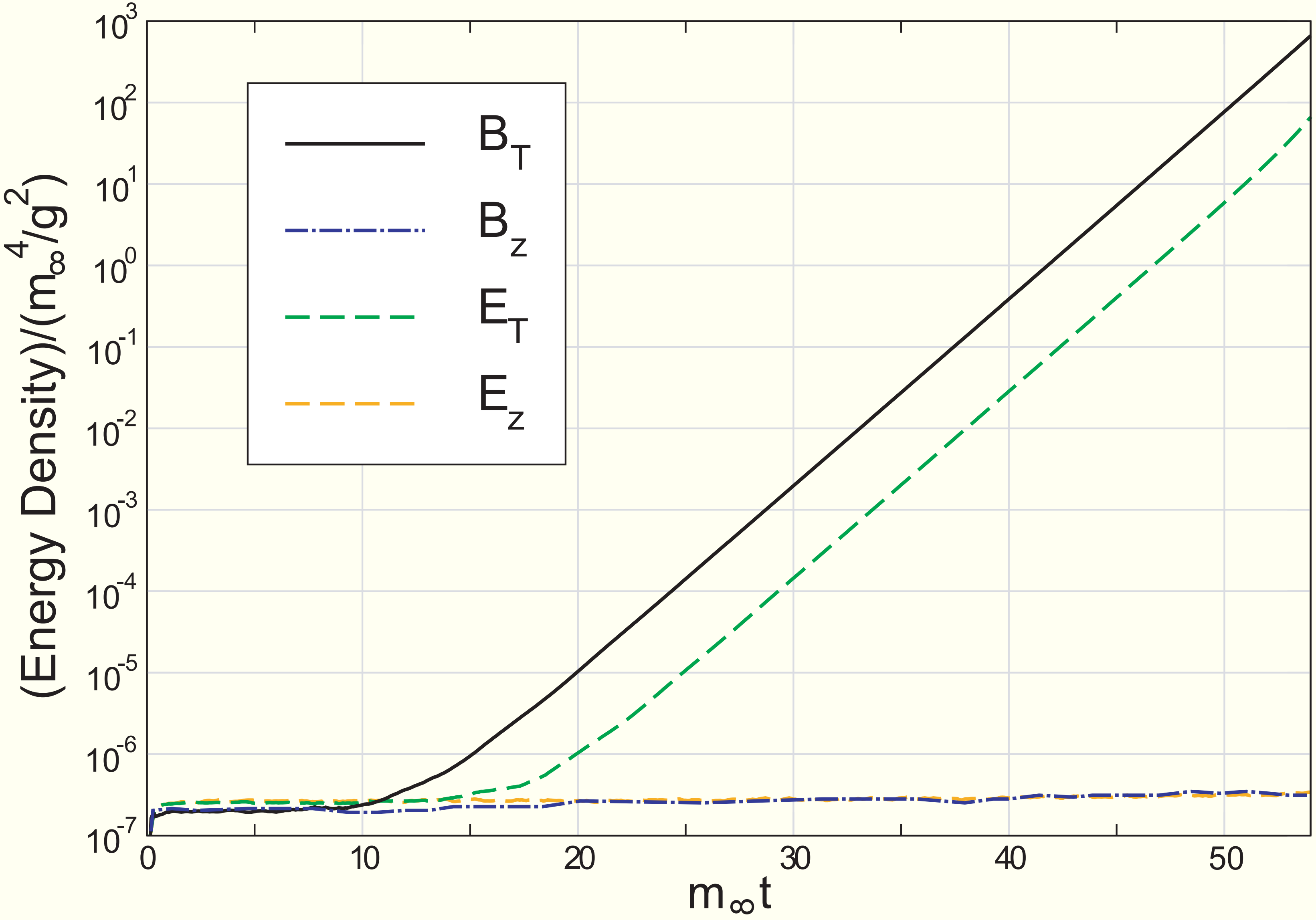

Collective Modes of an Isotropic QGP

The isotropic hard-thermal-loop (HTL) gluon propagator is given by

$$\Delta^{ij} = (k^2 - \omega^2 + \Pi_T)^{-1}(\delta_{ij} - k^i k^j / k^2) - \frac{k^2}{\omega^2}(k^2 - \Pi_L)^{-1} k^i k^j / k^2$$

with

$$\begin{aligned} \Pi_T(\omega, k) &= \frac{m_D^2}{2}\frac{\omega^2}{k^2}\left[1 - \frac{\omega^2 - k^2}{2\omega k}\log\frac{\omega + k}{\omega - k}\right] , \\ \Pi_L(\omega, k) &= m_D^2\left[\frac{\omega}{2k}\log\frac{\omega + k}{\omega - k} - 1\right] , \end{aligned}$$

and $m_D \propto gT$.

$$\begin{aligned} \lim_{\omega\to 0} \Pi_L(\omega, k) &= m_D^2 \quad \text{electric screening} \\ \lim_{\omega\to 0} \Pi_T(\omega, k) &= 0 \quad\quad \textbf{no} \text{ magnetic screening} \end{aligned}$$

Collective Modes of an Isotropic QGP

In the isotropic case the only poles are at real timelike ($\omega > k$) momentum. In order to determine the dispersion relations for these excitations we can then explicitly look for the poles in the propagator.

$$
\begin{aligned}
0 &= k^2 - \omega_T^2 + \Pi_T(\omega_T, k) \\
0 &= k^2 - \Pi_L(\omega_L, k)
\end{aligned}
$$

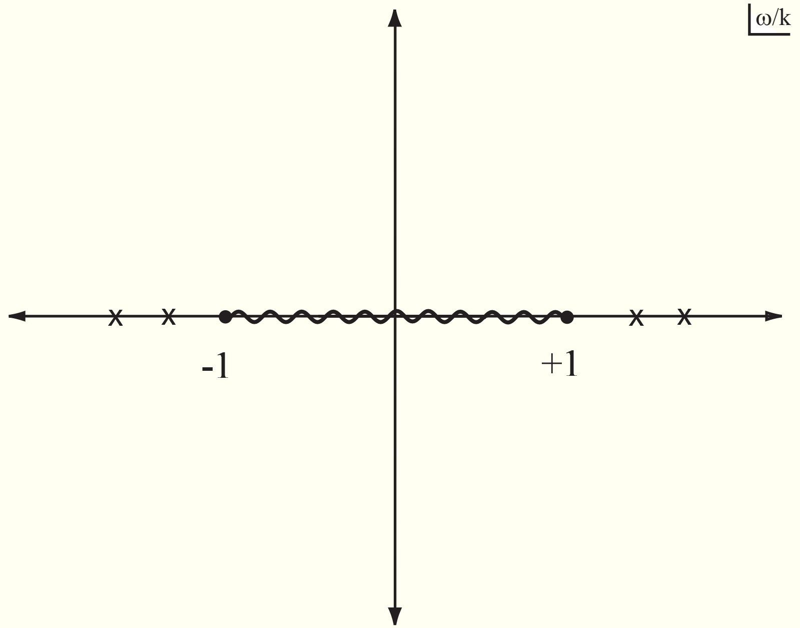

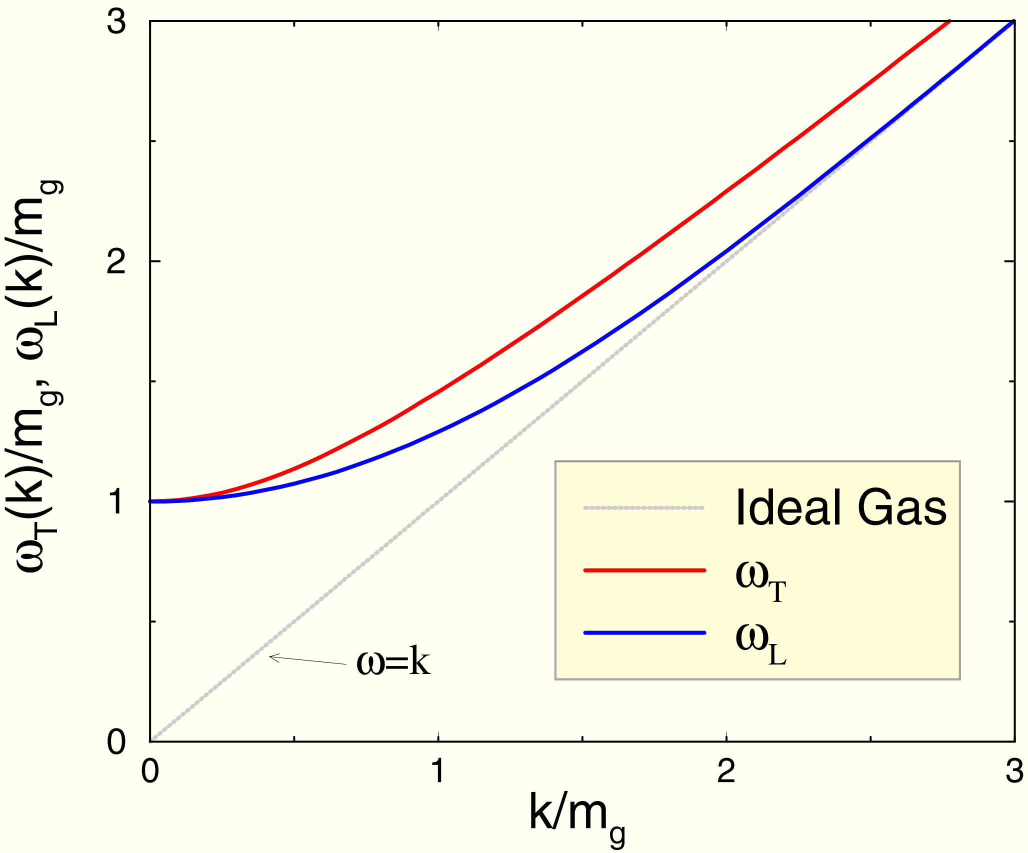

Anisotropic Gluon Polarization Tensor

In order to determine the HL gluon polarization we can use either linearized three-dimensional kinetic theory (Boltzmann-Vlasov eq)

$$[v \cdot D_X, \delta f(p,X)] + g v_\mu F^{\mu\nu}(X)\partial_\nu^{(p)} f(\mathbf{p}) = 0$$

$$D_\mu F^{\mu\nu} = J^\nu = g \int_p v^\nu \delta f(p,X)$$

or diagrammatically

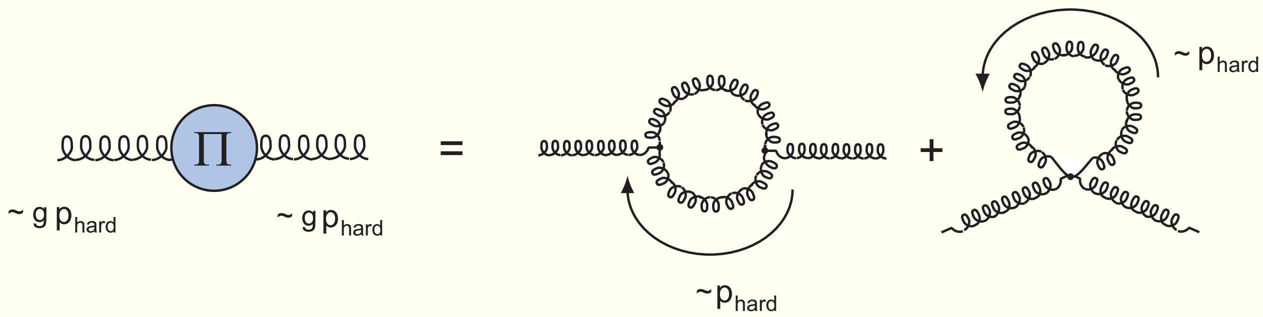

In both cases the result for the retarded self-energy is

$$\Pi^{ij}_{ab}(K) = -g^2 \delta_{ab} \int_{\mathbf{p}} v^i \partial_l f(\mathbf{p}) \left(\delta^{jl} - \frac{v^j k^l}{K \cdot V + i\epsilon} \right)$$

The nature of the anisotropy

We assume that the anisotropic distribution function can be obtained from an arbitrary isotropic distribution function by a change of its argument.

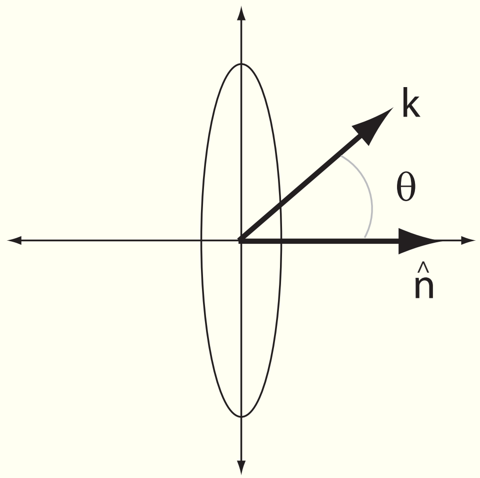

$$f(p^2) \to f(p^2 + \xi(p \cdot n)^2)$$

The polarization tensor can then be written as

$$\Pi^{ij}(K) = m_D^2 \int \frac{d\Omega}{4\pi} v^i \frac{v^l + \xi(v \cdot n)n^l}{(1 + \xi(v \cdot n)^2)^2} \left(\delta^{jl} - \frac{v^j k^l}{K \cdot V + i\epsilon} \right)$$

where m_D is the *isotropic* Debye mass

$$m_D^2 = -\frac{g^2}{2\pi^2} \int_0^\infty dp\, p^2 \frac{df(p^2)}{dp}$$

P. Romatschke and MS, hep-ph/0304092.

New Mass Scales – $\xi > 0$

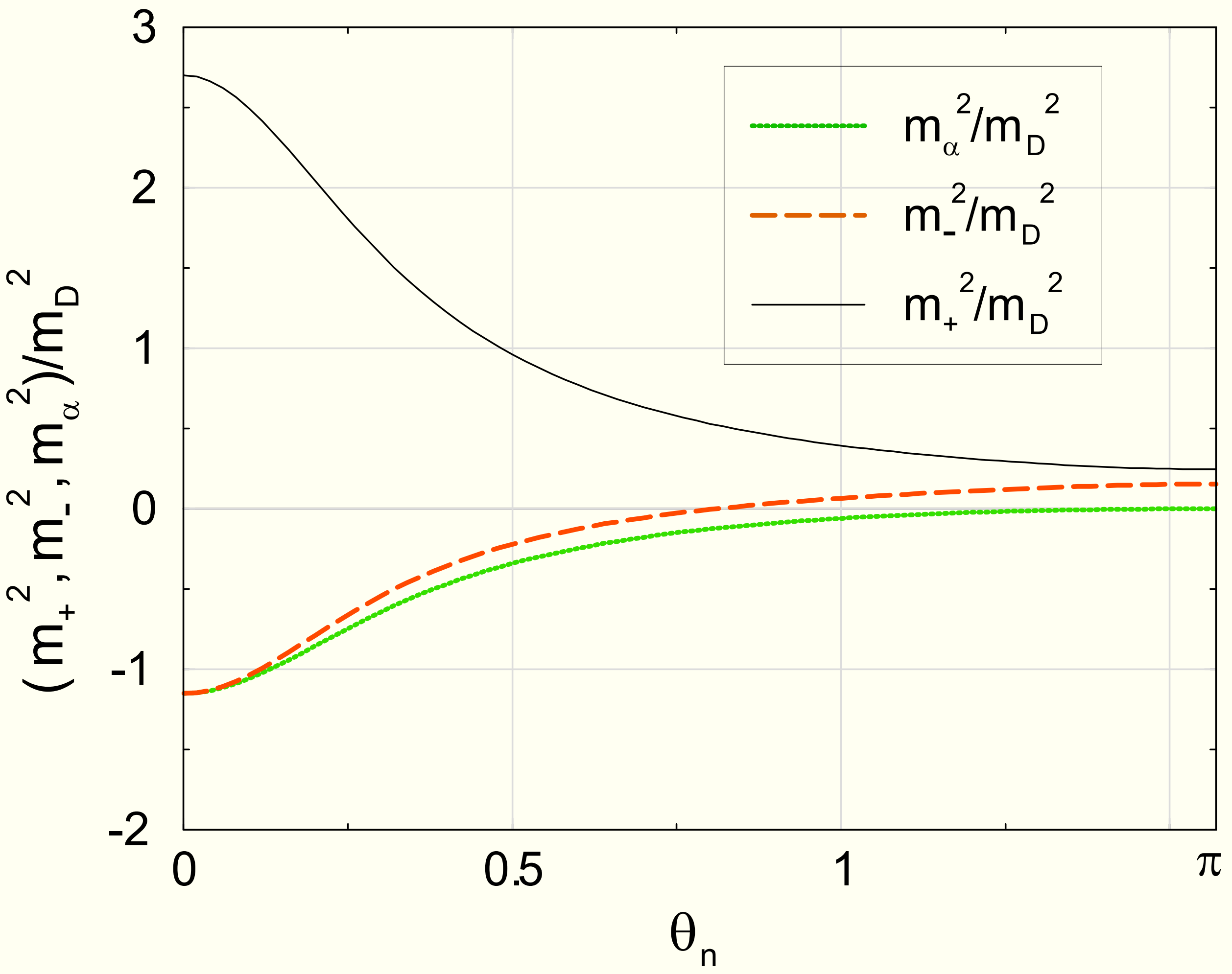

Angular dependence of m_α^2, m_+^2, and m_-^2 at fixed $\xi = 10$.

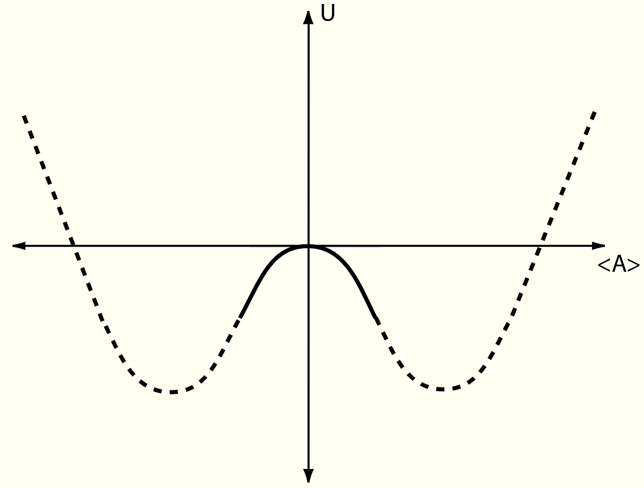

Sketch of the effective potential of an unstable mode.

Anisotropic Collective Modes ($\xi > 0$)

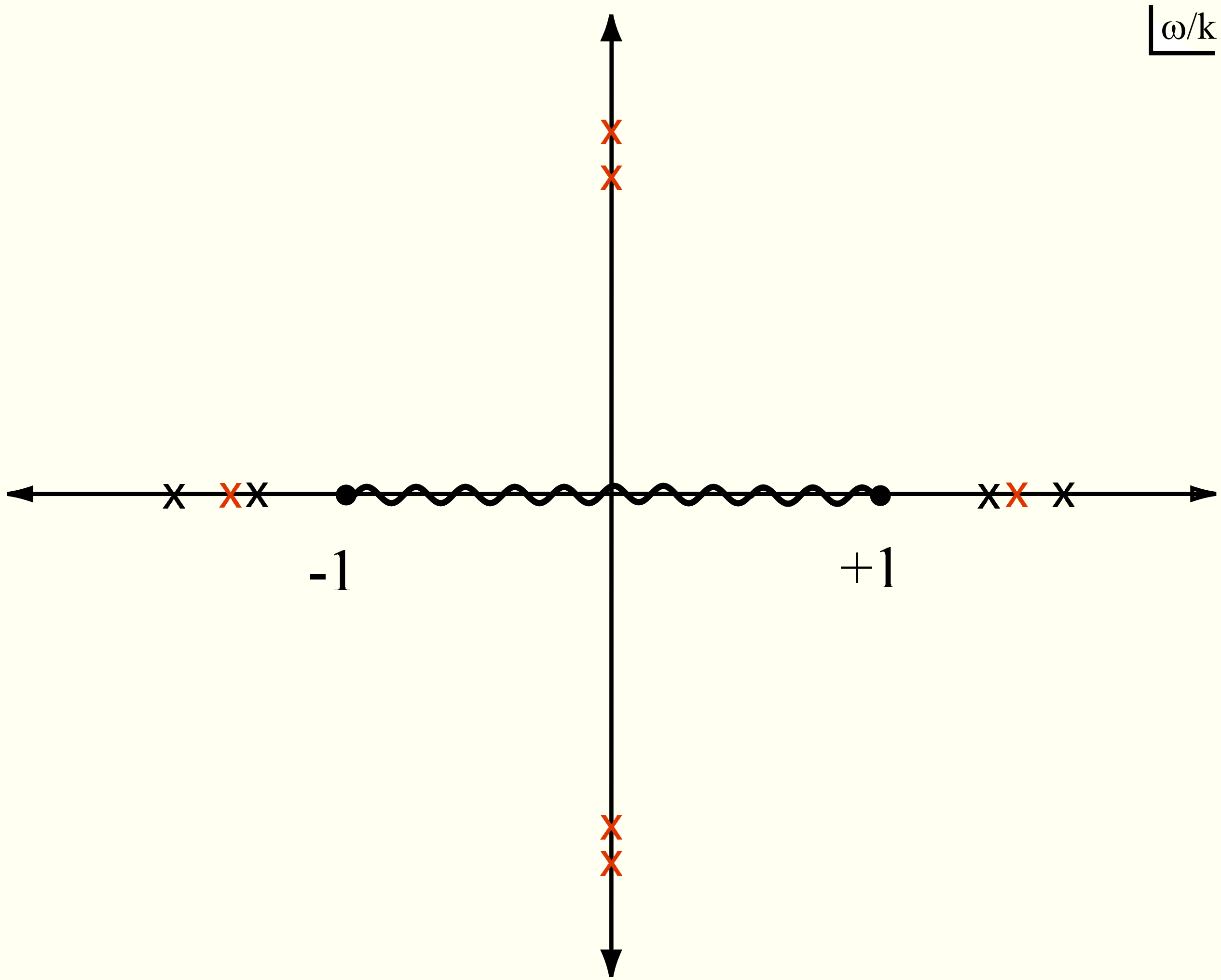

Anisotropic poles ($\xi > 0$).

Unstable Modes – $\xi > 0$

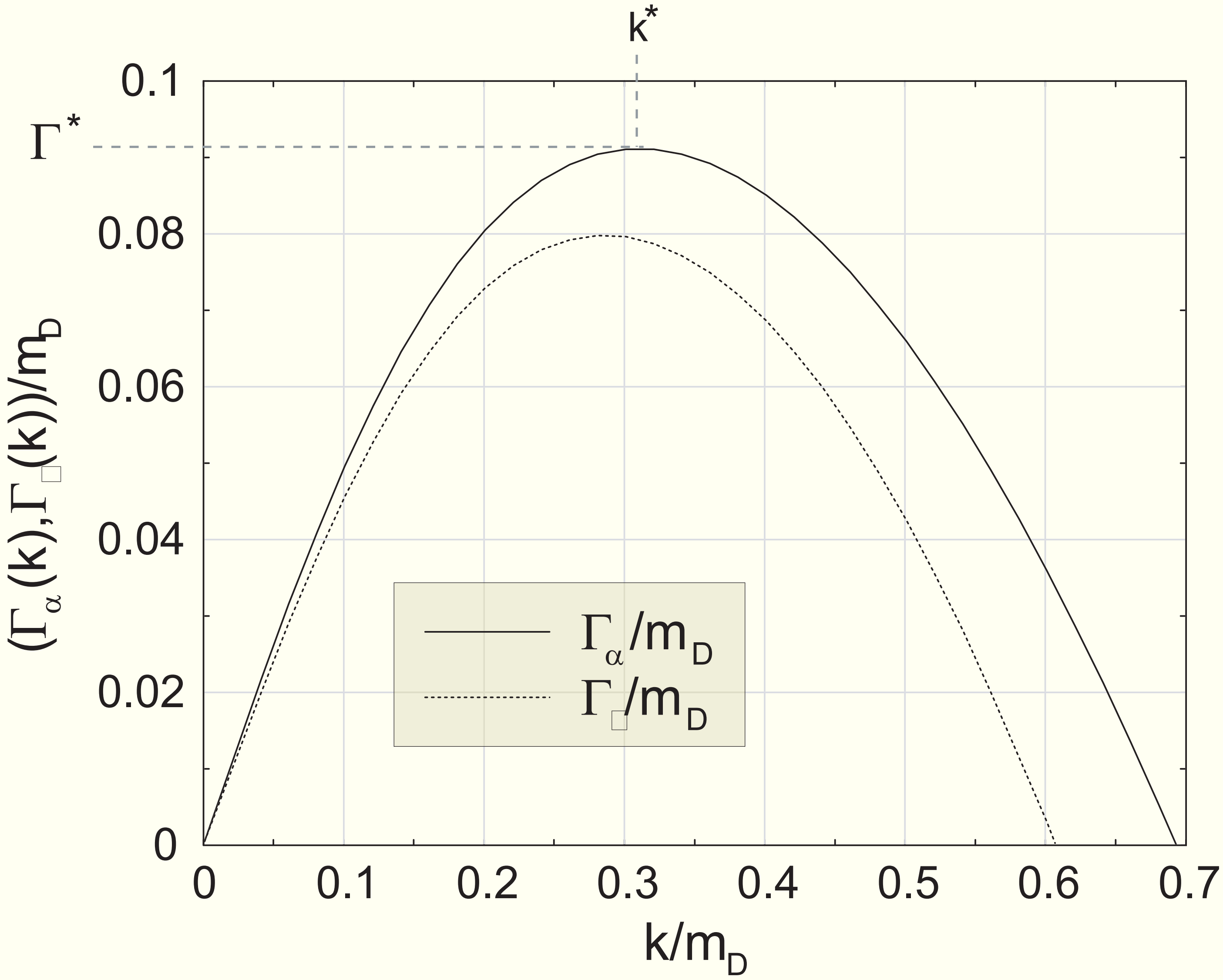

$\Gamma_\alpha(k)$ and $\Gamma_-(k)$ as a function of k for $\xi = 10$ and $\theta_n = \pi/8$.

Unstable Modes Cartoon – Increasing ξ

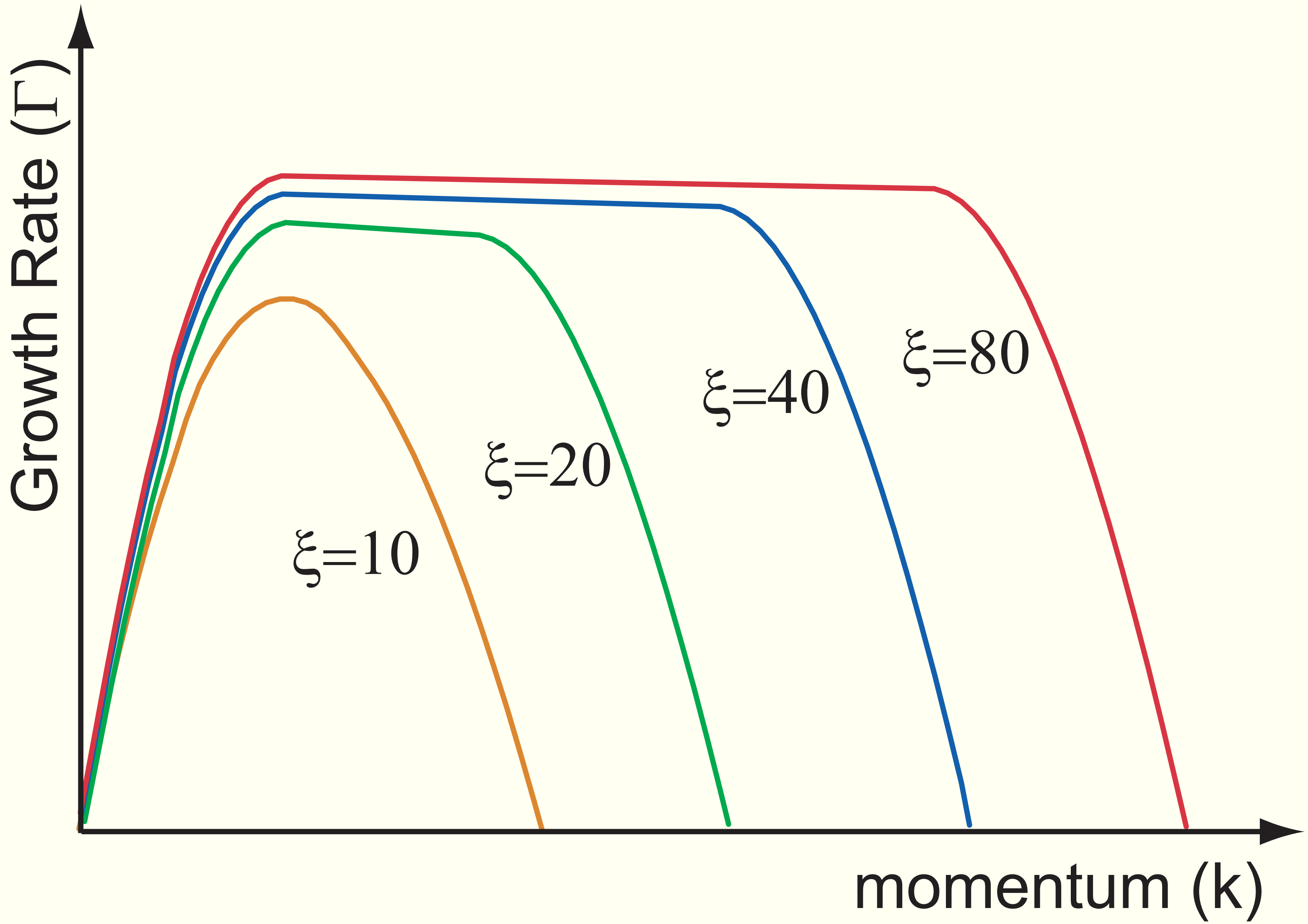

Anisotropic HL Effective Action

Using the requirement of gauge invariance it is possible to determine all n-point functions.

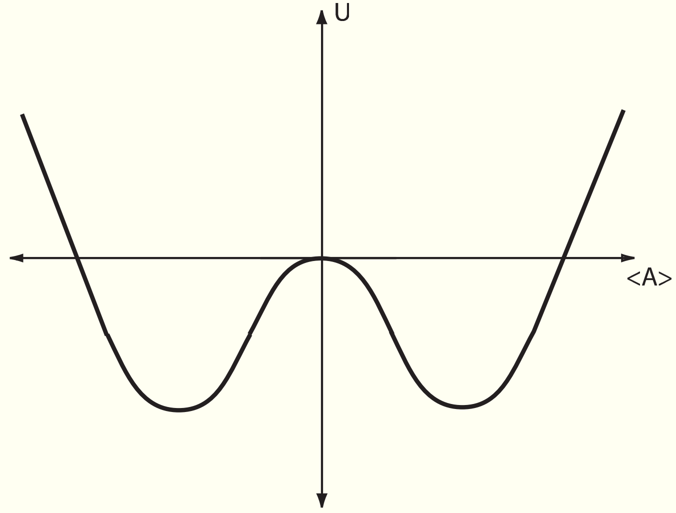

$$
\begin{aligned}
S_{\mathrm{HL}} &= -\frac{g^2}{2}\int_x \int_{\mathbf{p}} f(\mathbf{p})\, F^a_{\mu\nu}(x) \left(\frac{p^\nu p^\rho}{(p\cdot D)^2} \right)_{ab} F_\rho{}^{b\,\mu}(x) \\
&= -\frac{g^2}{2}\int_x \int_{\mathbf{p}} f(\mathbf{p})\, W^\mu(x,\hat{\mathbf{p}}) W_\mu(x,\hat{\mathbf{p}})
\end{aligned}
$$

For example, from this we can obtain the anisotropic 3-gluon vertex

$$
\Gamma^{\mu\nu\lambda}(k,q,r) = \frac{g^2}{2}\int_{\mathbf{p}} \frac{\partial f(\mathbf{p})}{\partial p^\beta}\, \hat{p}^\mu \hat{p}^\nu \hat{p}^\lambda \left(\frac{r^\beta}{\hat{p}\cdot q\ \hat{p}\cdot r} - \frac{k^\beta}{\hat{p}\cdot k\ \hat{p}\cdot q} \right)
$$

Real-Time Lattice Simulation

Numerically solve the equations of motion resulting from the HL effective action on a space + velocity lattice.

$$j^\mu[A] = -g^2 \int_{\mathbf{p}} \frac{1}{2|\mathbf{p}|}\, p^\mu\, \frac{\partial f(\mathbf{p})}{\partial p^\beta} W^\beta(x;\mathbf{v})$$

with

$$[v \cdot D(A)] W_\beta(x;\mathbf{v}) = F_{\beta\gamma}(A) v^\gamma$$

and $v^\mu = p^\mu/|\mathbf{p}| = (1, \mathbf{v})$.

This has to be solved with

$$D_\mu(A) F^{\mu\nu} = j^\nu$$

where $\nu = 0$ is the Gauss law constraint.

$\vec{\mathrm{v}}$-discretized equations of motion

Recall,

$$j^\nu[A] = -g^2 \int_{\mathbf{p}} \frac{1}{2|\mathbf{p}|}\, p^\nu \,\frac{\partial f(\mathbf{p})}{\partial p^\beta} W^\beta(x;\mathbf{v})$$

A closed set of gauge-covariant equations is obtained when the angular integral over $\hat{\mathbf{p}}$ is discretized.

The full HL dynamics is then approximated by the following set of equations

$$[v\cdot D(A)]\mathcal{W}_{\mathbf{v}} = (a_{\mathbf{v}}F^{0\mu} + b_{\mathbf{v}}F^{z\mu})v_\mu$$
$$D_\mu(A)F^{\mu\nu} = j^\nu = \frac{1}{\mathcal{N}}\sum_{\mathbf{v}} v^\nu \mathcal{W}_{\mathbf{v}}$$

which can be systematically improved by increasing $\mathcal{N}$.

Hard-loop results – $\xi = 10$ – Weak Anisotropy

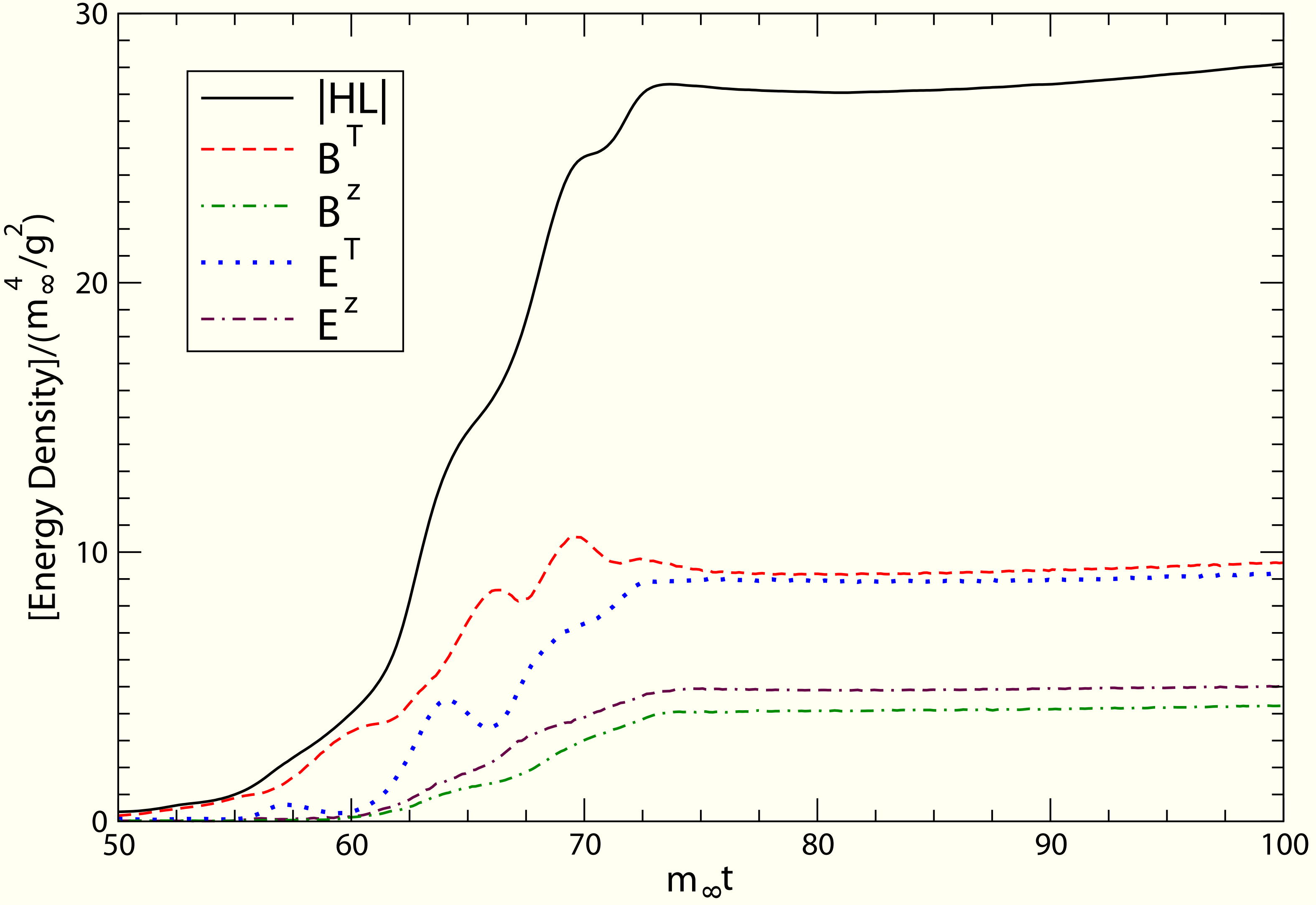

A. Rebhan, P. Romatschke, M. Strickland, hep-ph/0505261

Hard-loop results – Nonabelian cascade – $\xi = 10$

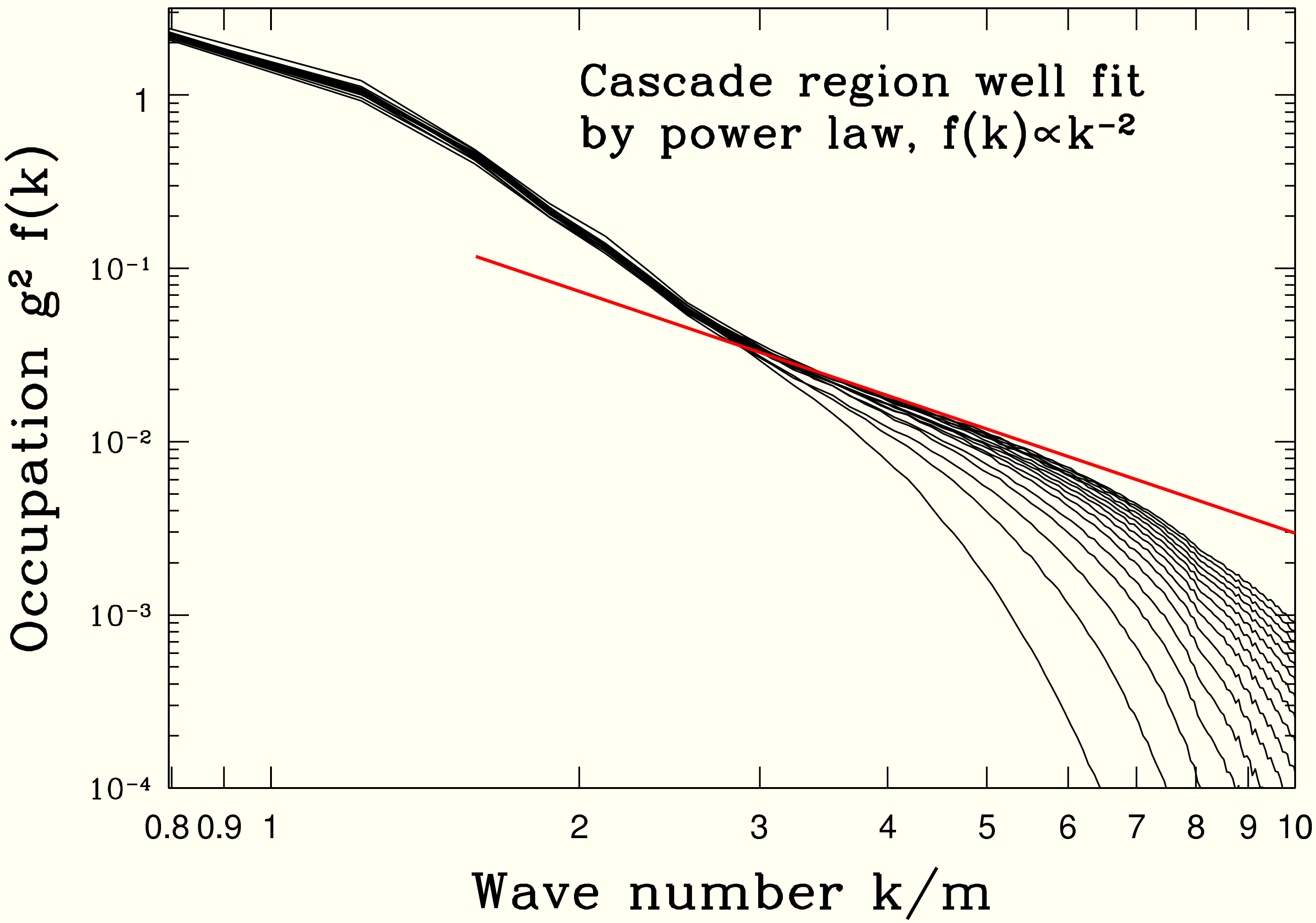

“Kolmogorov turbulence”

P. Arnold and G. Moore, hep-ph/0509206; hep-ph/0509226.

Larger Anisotropies - $\xi = 100$

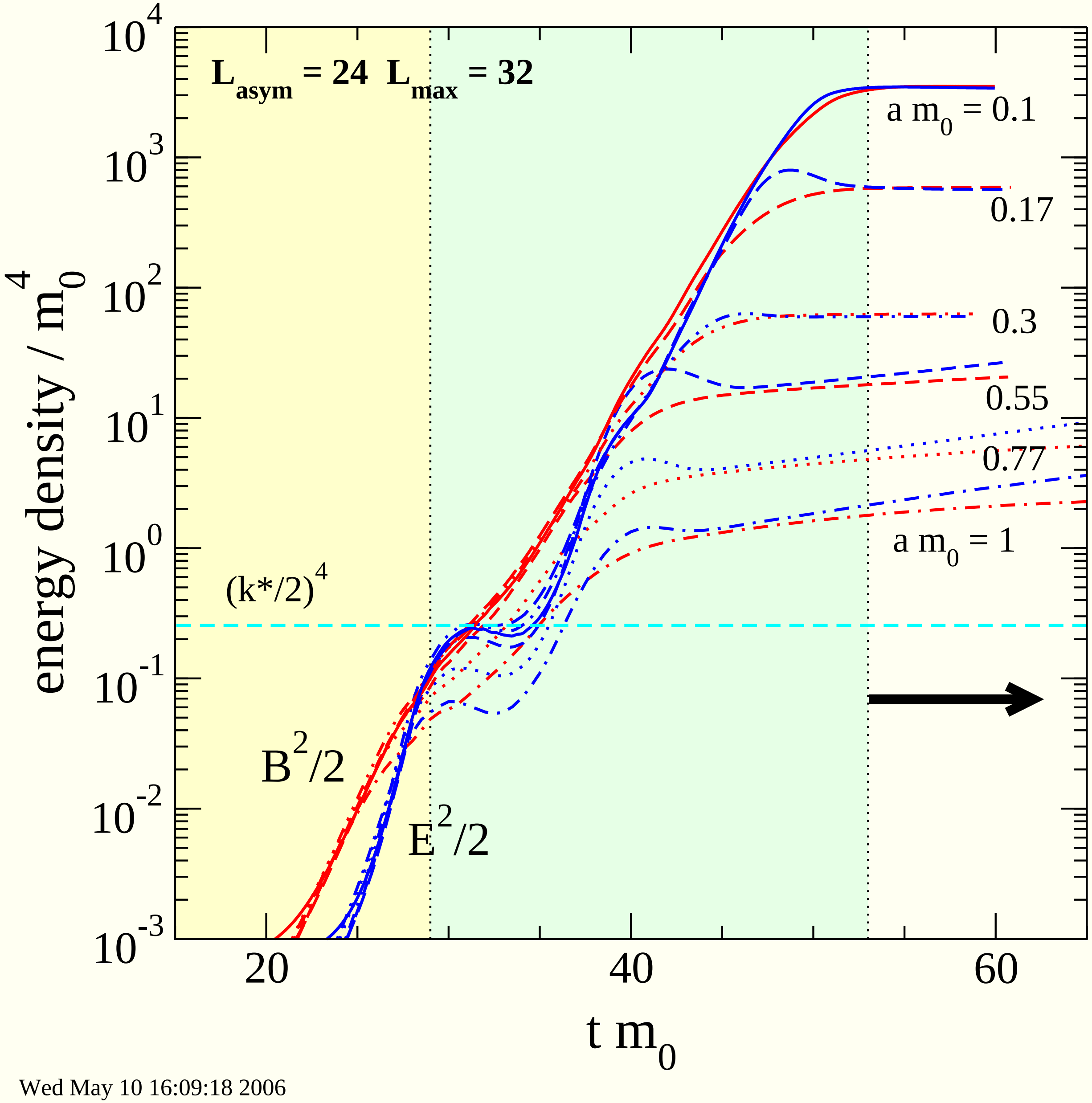

D. Bödeker and K. Rummukainen, forthcoming.

240^3 Lattice with up to 14250 W fields per site!

Colored-Particle-in-Cell Simulations (CPIC)

Hard-loop approximation strictly only applies when we ignore the back-reaction of the particles on the background field.

What happens when one relaxes this assumption? Let's go back to the transport equations and try to solve without linearization. Recall the Vlasov equation

$$p^\mu [\partial_\mu - g q^a F^a_{\mu\nu} \partial^\nu_p - g f_{abc} A^b_\mu q^c \partial_{q^a}] f(x,p,q) = 0$$

The Vlasov equation is coupled self-consistently to the Yang-Mills equation for the soft gluon fields,

$$D_\mu F^{\mu\nu} = J^\nu = g \int \frac{d^3 p}{(2\pi)^3} dq \, q \, v^\nu f(t, \boldsymbol{x}, \boldsymbol{p}, q)$$

A. Dumitru, Y. Nara, and MS, hep-ph/0604149

CPIC - Wong-Yang-Mills equations

Can be solved numerically by replacing the continuous single-particle distribution $f(\boldsymbol{x},\boldsymbol{p},q)$ by a large number of test particles:

$$f(\boldsymbol{x},\boldsymbol{p},q) = \frac{1}{N_{\rm test}} \sum_i \delta(\boldsymbol{x}-\boldsymbol{x}_i(t))\,(2\pi)^3 \delta(\boldsymbol{p}-\boldsymbol{p}_i(t))\,\delta(q^a - q_i^a(t))$$

where $\boldsymbol{x}_i(t)$, $\boldsymbol{p}_i(t)$ and $q_i^a(t)$ are the coordinates, momentum, and charge of an individual test particle.

$$\begin{aligned}
\frac{d\boldsymbol{x}_i}{dt} &= \boldsymbol{v}_i \\
\frac{d\boldsymbol{p}_i}{dt} &= g\, q_i^a\, (\boldsymbol{E}^a + \boldsymbol{v}_i \times \boldsymbol{B}^a) \\
\frac{d\boldsymbol{q}_i}{dt} &= ig\, v_i^\mu\, [A_\mu, \boldsymbol{q}_i] \\
J^{a\,\nu} &= \frac{g}{N_{\rm test}} \sum_i q_i^a\, v^\nu\, \delta(\boldsymbol{x}-\boldsymbol{x}_i(t))
\end{aligned}$$

CPIC - Point Particle Method

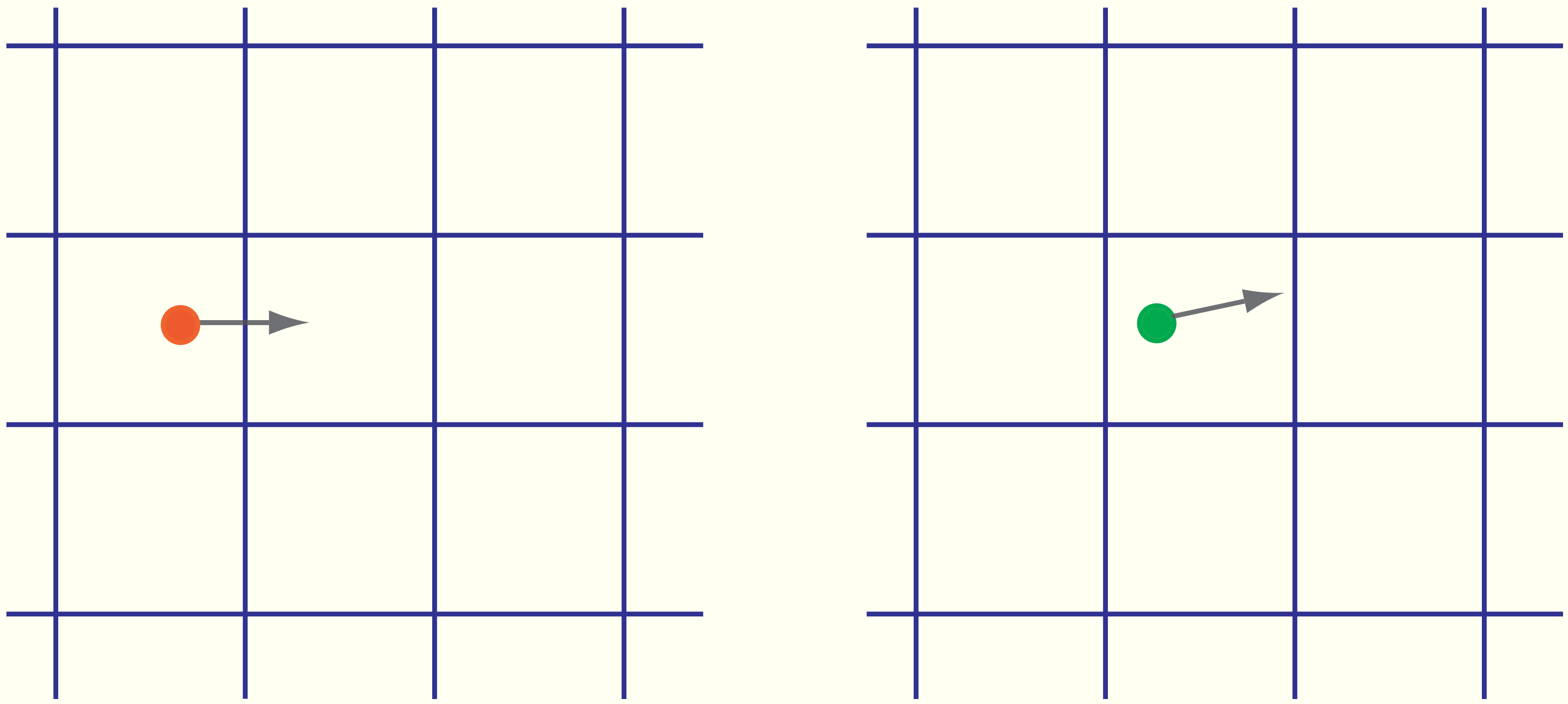

Cartoon picture of a point-like colored test-particle crossing a cell boundary.

Unfortunately for a stable 3d particle-in-cell tens of thousands of pointlike test-particles per cell are required! This makes this method difficult (if not impossible) to implement numerically.

Need a better method . . .

CPIC - Smeared color particles

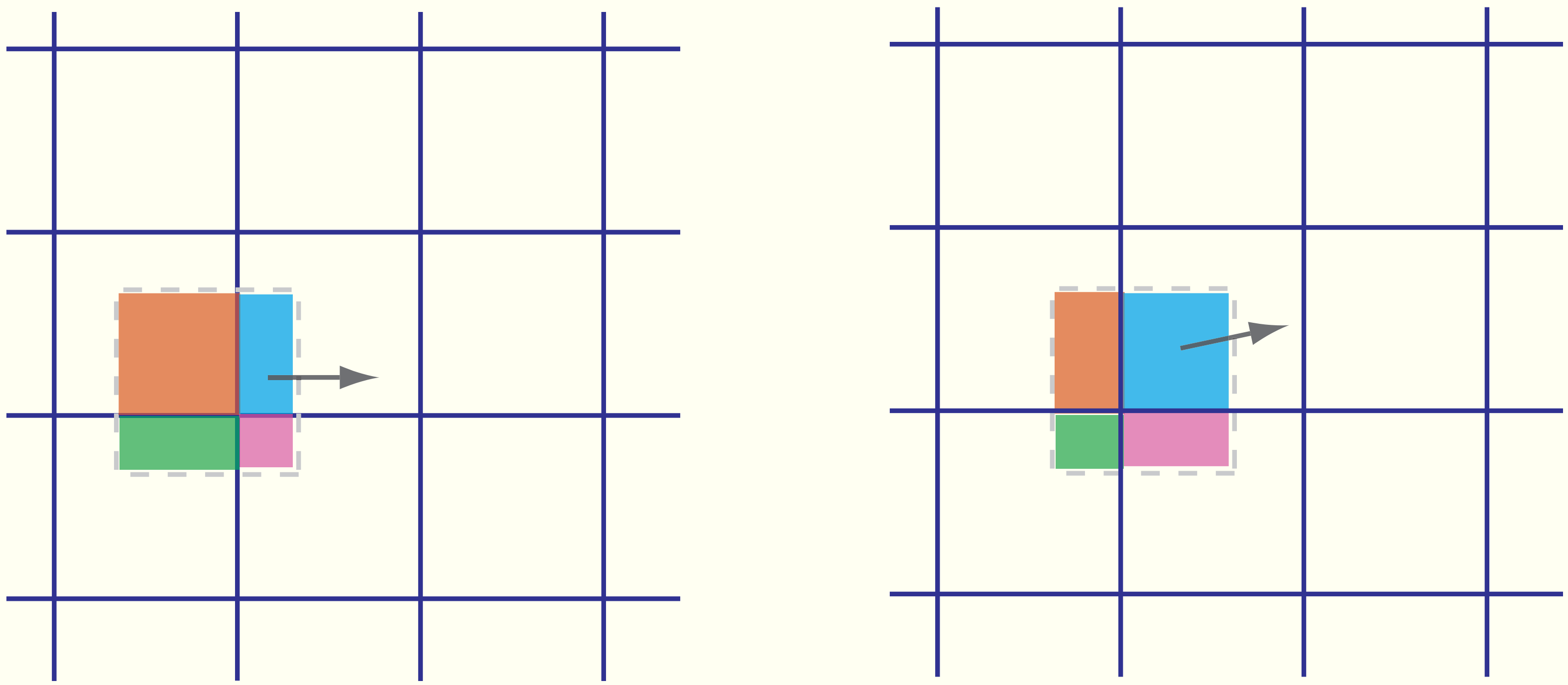

Cartoon picture of “smeared” colored test-particle crossing a cell boundary.

With this method, convergent results are achieved with as few 20 smeared test-particles per cell!

CPIC - Highly anisotropic initial particle distribution

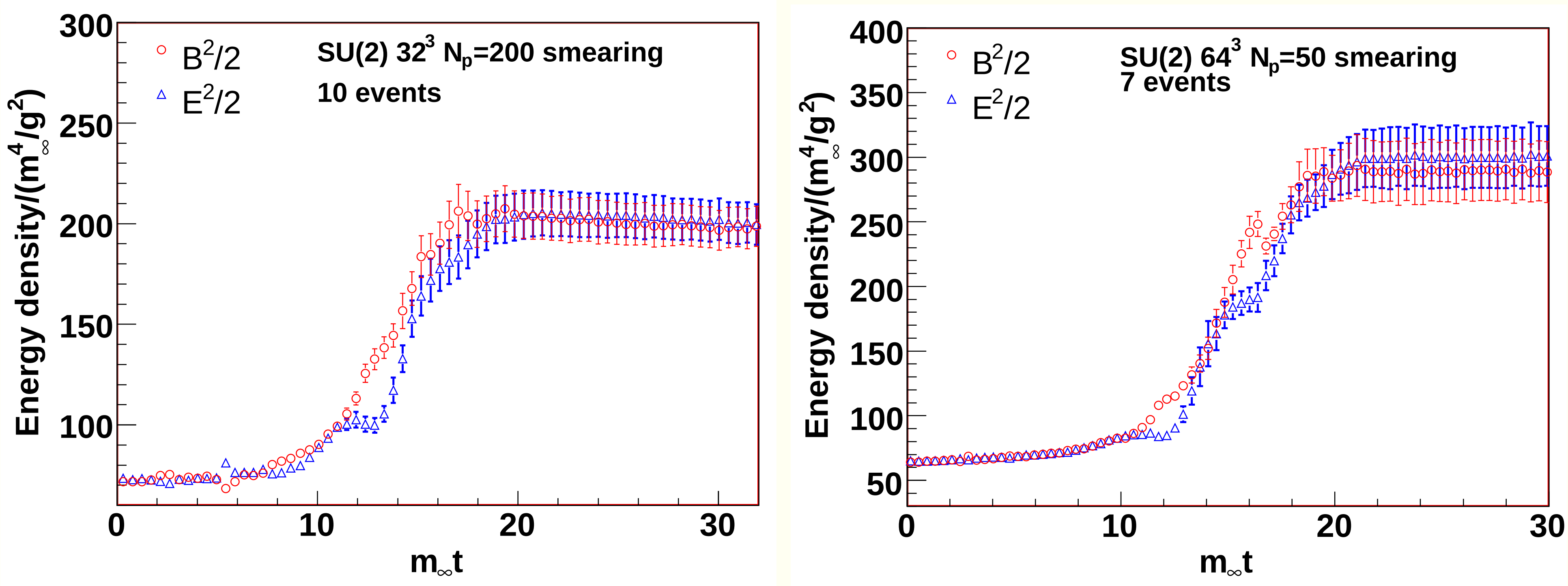

$L = 5$ fm, $p_{\rm hard} = 16$ GeV, $g^2\, n_g = 10/\text{fm}^3$, $m_\infty = 0.12$ GeV.

Saturated energy density increases as continuum limit is approached!
Final field configurations are isotropic.

CPIC - Ultraviolet Avalanche

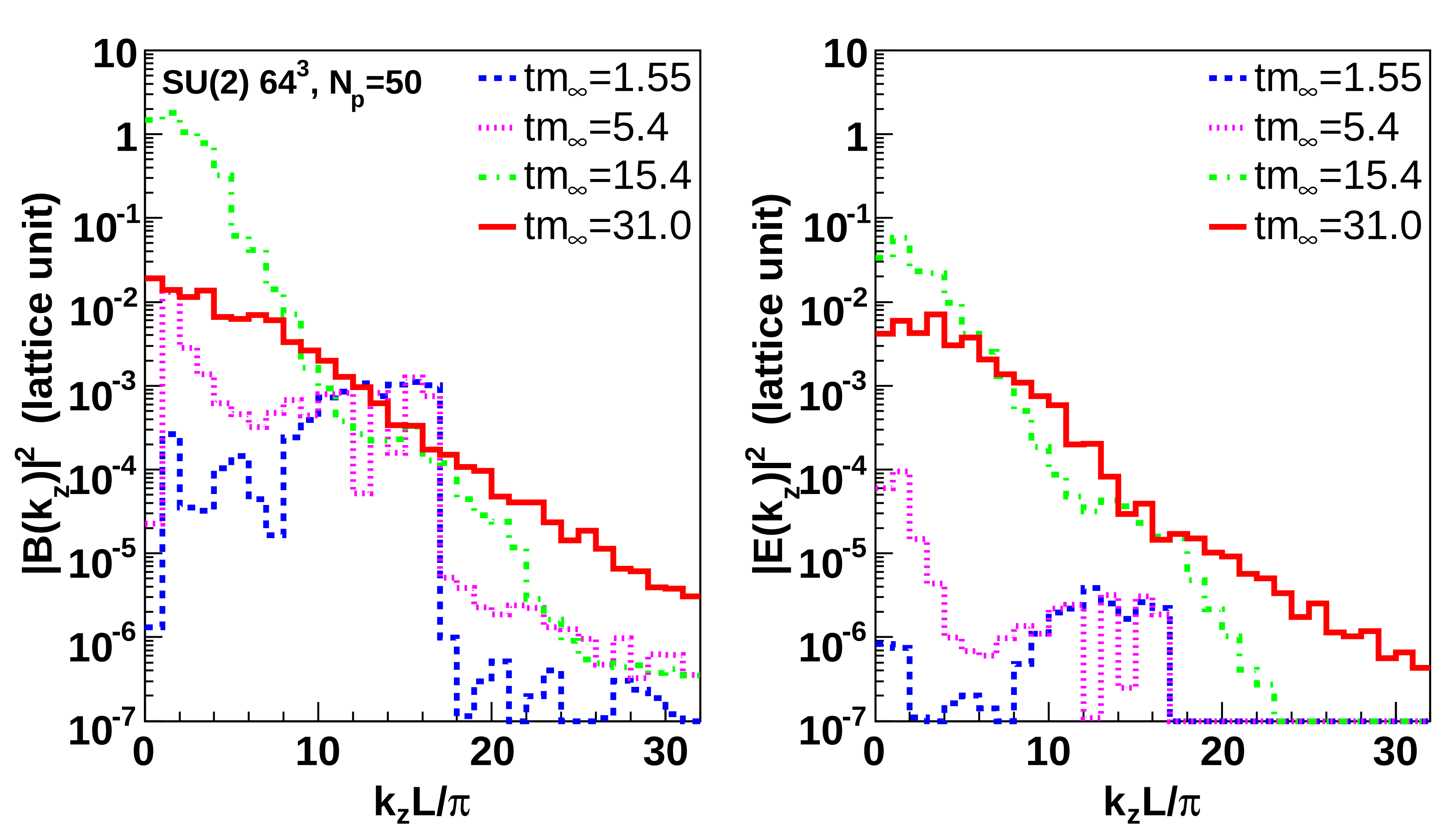

Squares of the Fourier transformed color-electric and color-magnetic fields at four different times.

Cycle of isotropization? - Initialize field modes

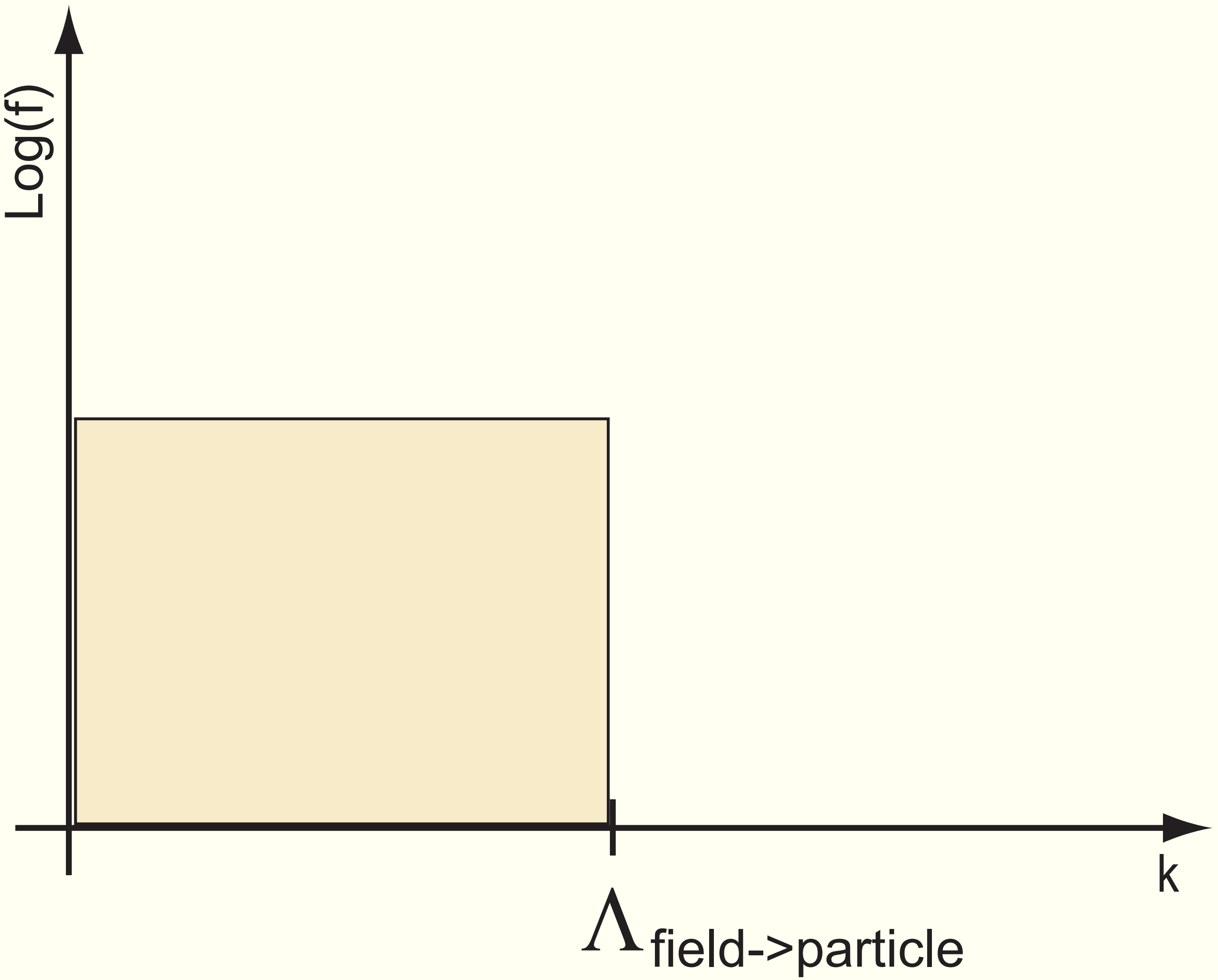

Cycle of isotropization? - Unstable modes grow

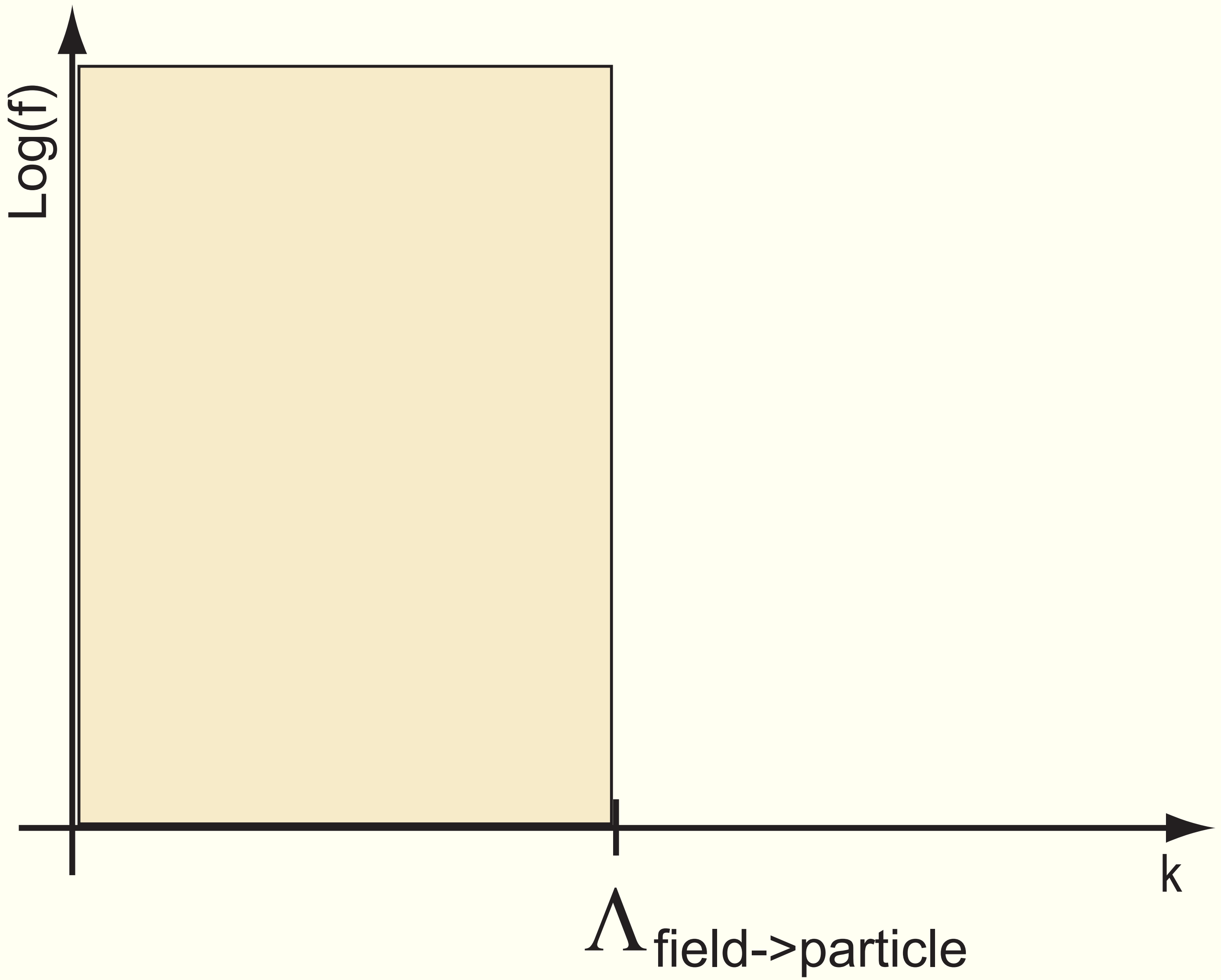

Cycle of isotropization? - Prepare for avalanche

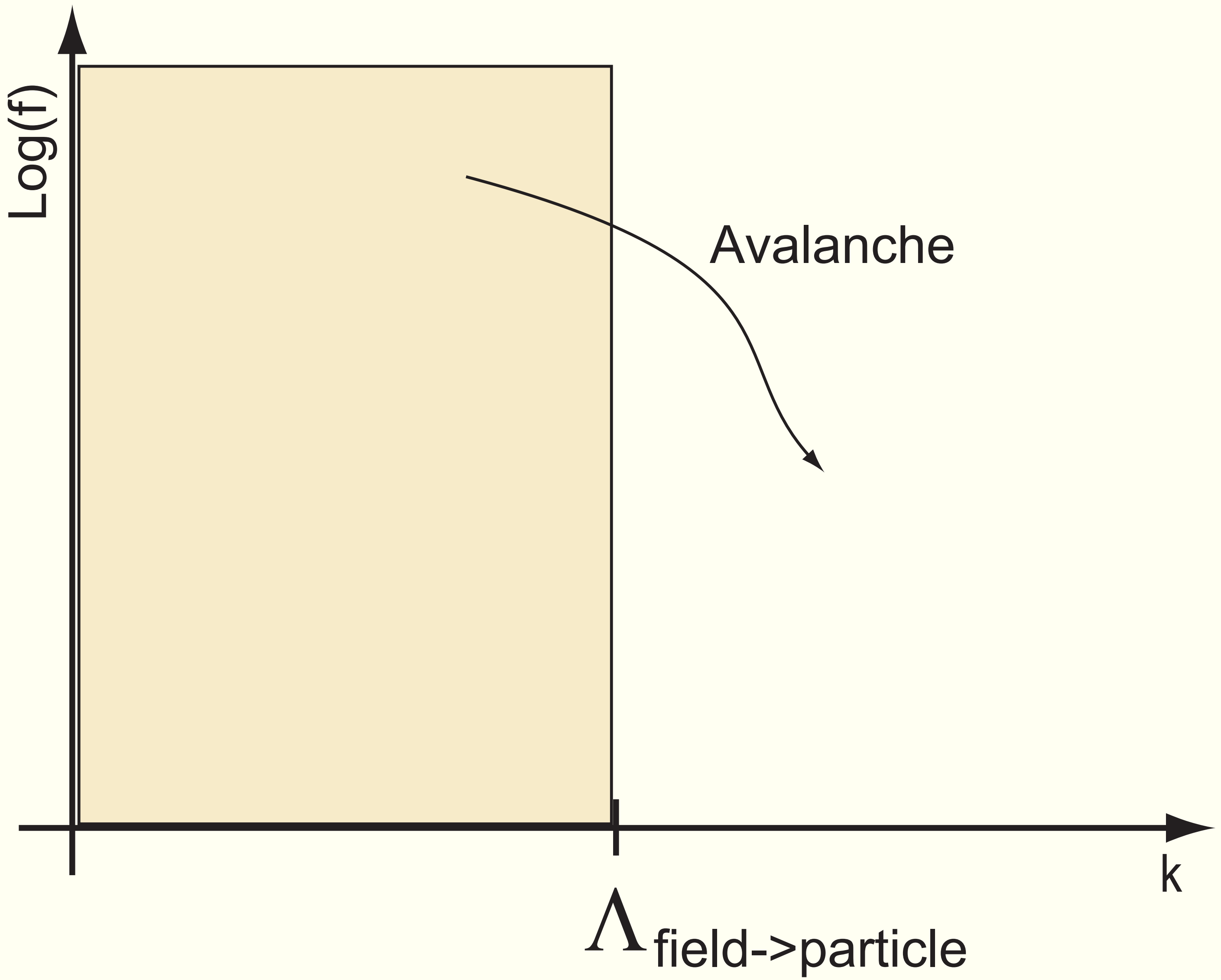

Cycle of isotropization? - After avalanche

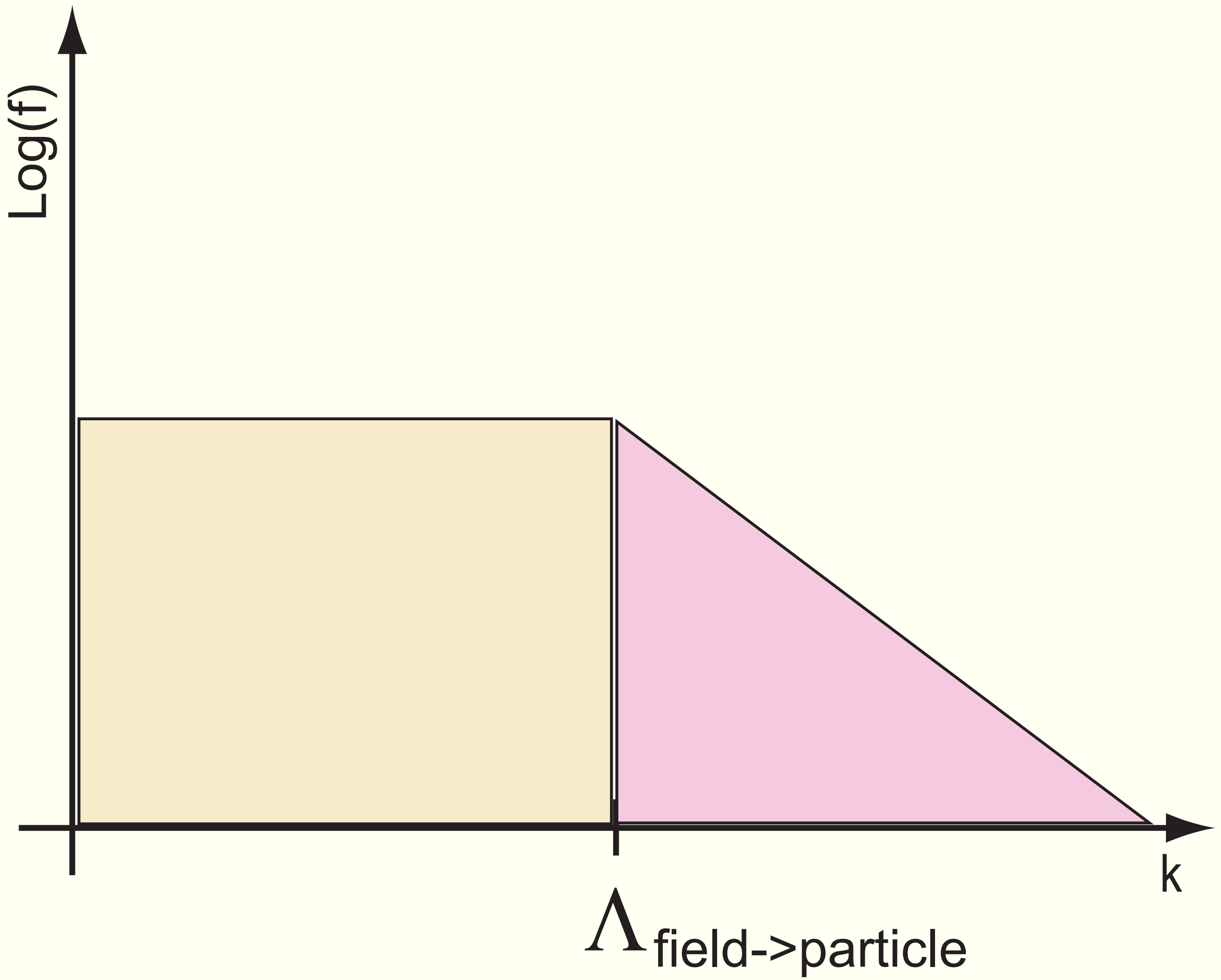

Cycle of isotropization? - Reshuffle and play again!

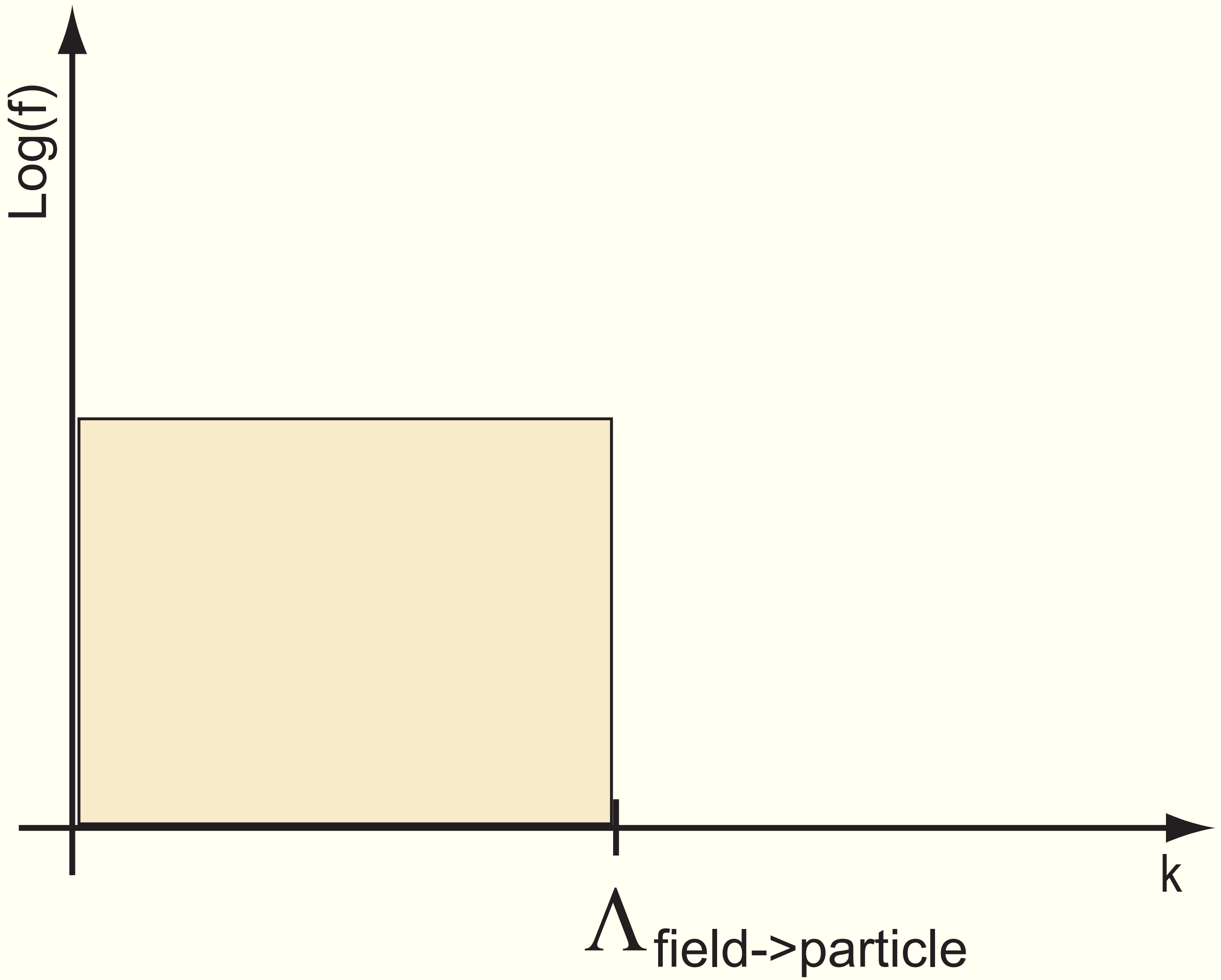

Cycle of isotropization? - Unstable modes grow

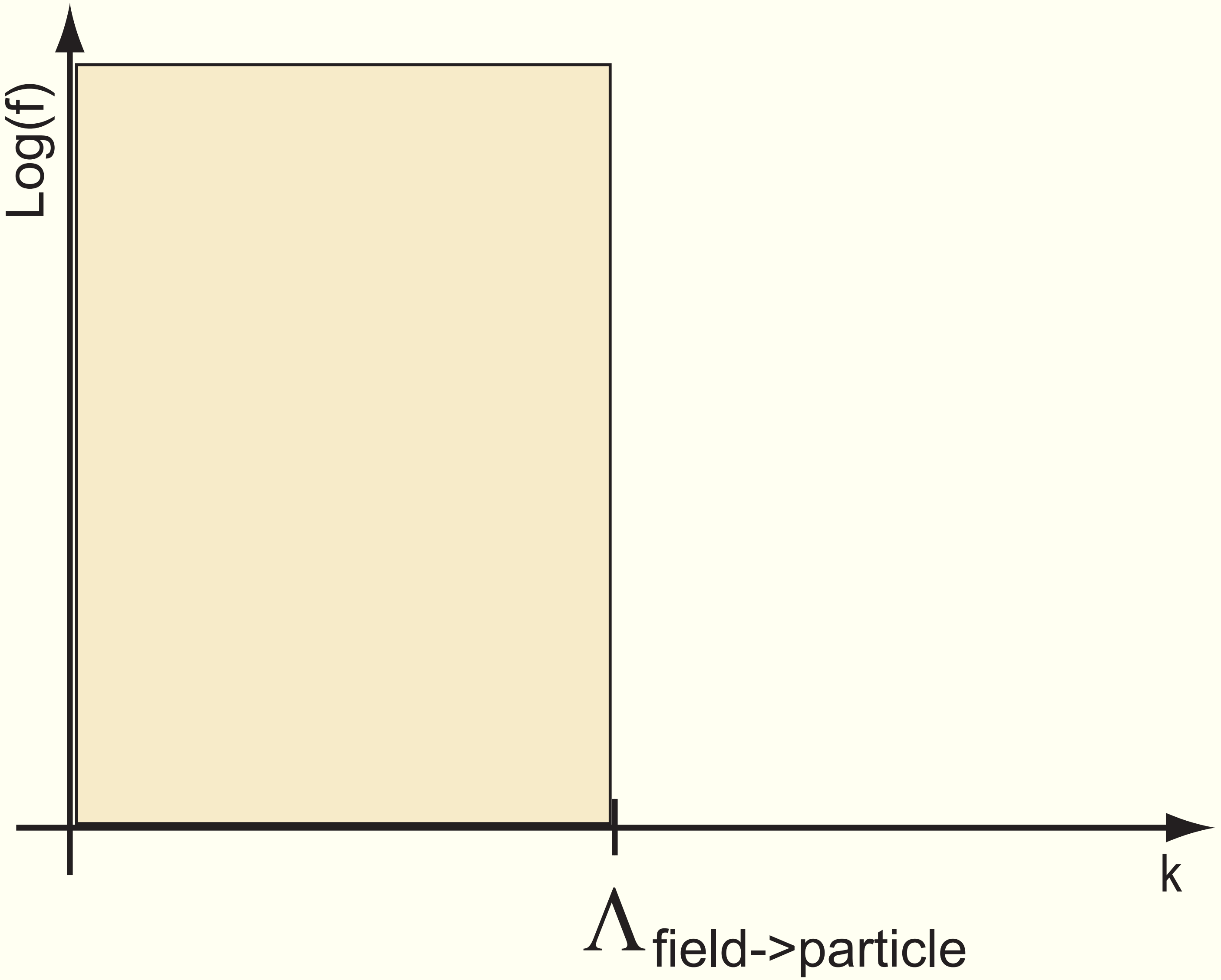

Cycle of isotropization? - Prepare for avalanche

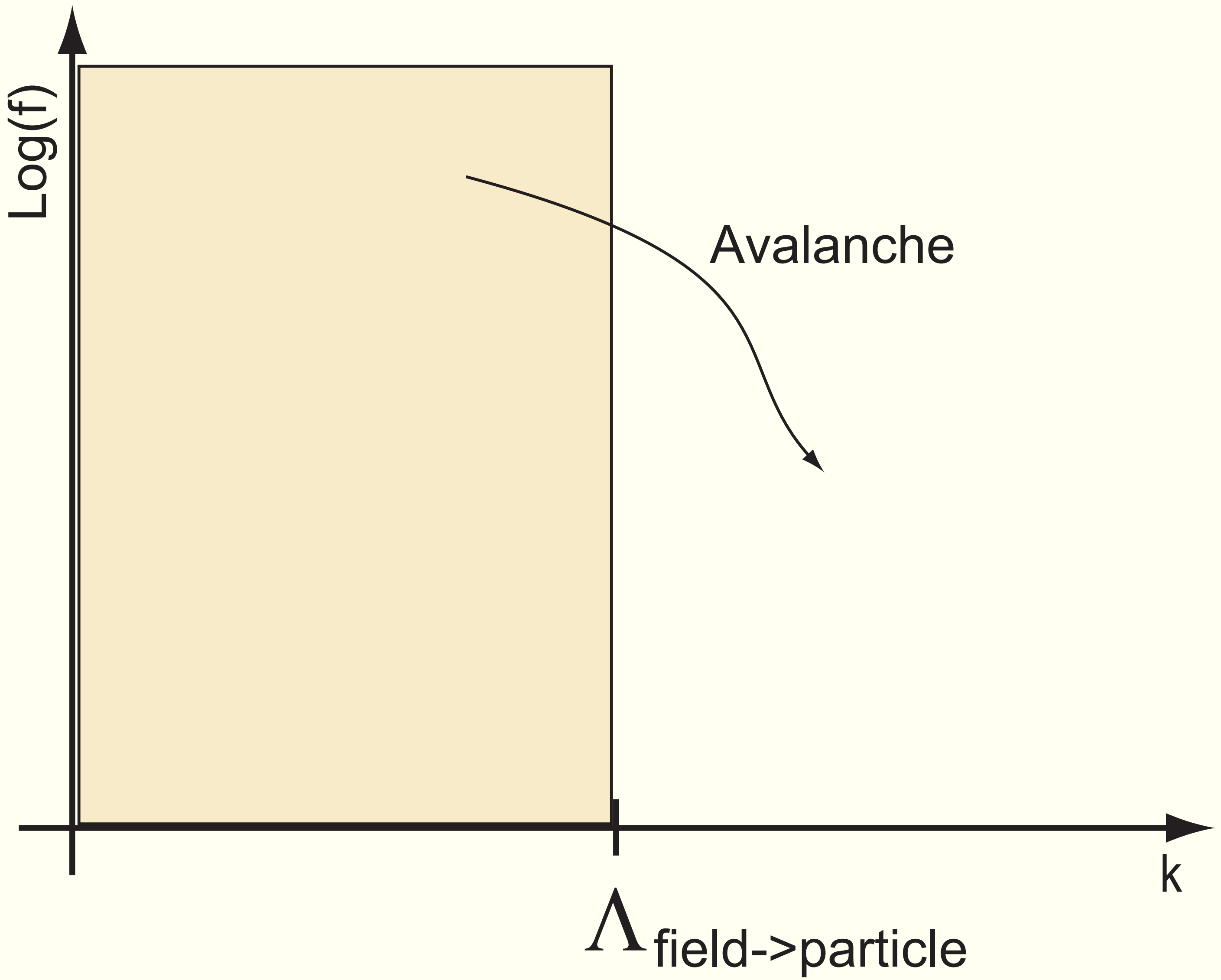

Cycle of isotropization? - After avalanche

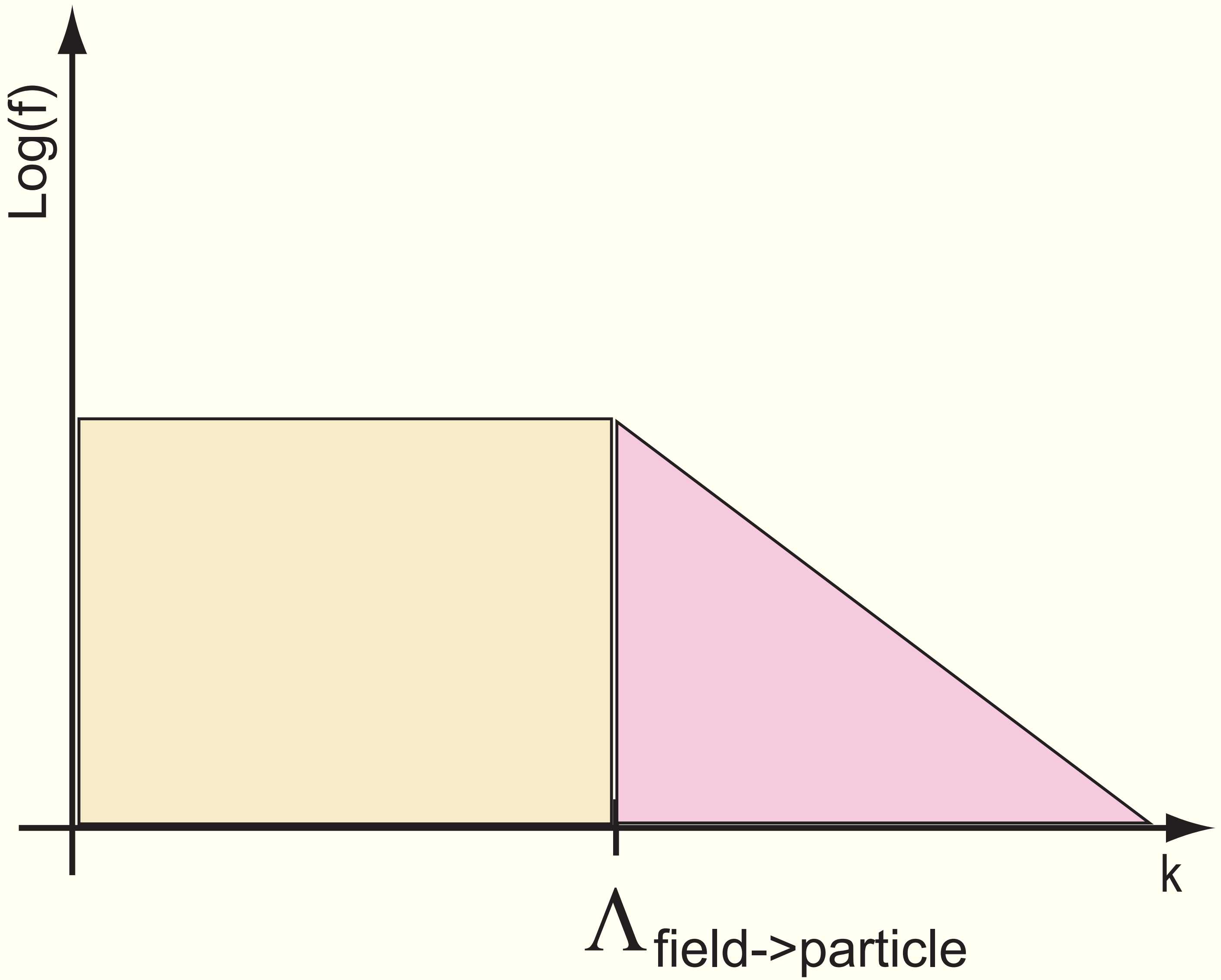

Cycle of isotropization? - Reshuffle and play again!

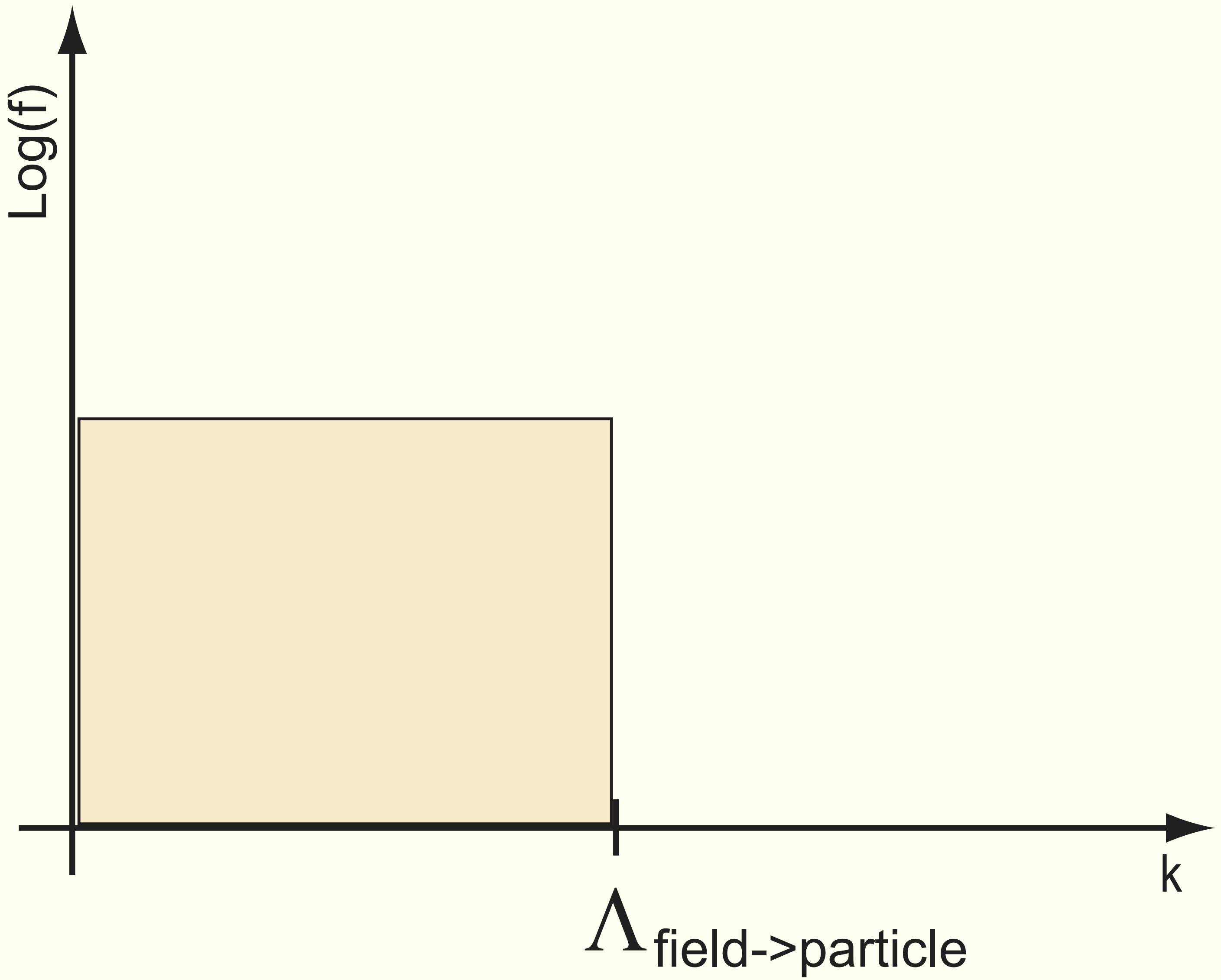

Other things to note

- Instability is also observed in classical CGC simulations which include longitudinal momentum space fluctuations $\rightarrow$ CGC is unstable! [P. Romatschke, R. Venugopalan, hep-ph/0605045]
- It is possible to solve the transport equations in an expanding system in order find exactly where the expansion and instability growth rate balance. [A. Rebhan and P. Romatschke, hep-ph/0605064]
- Anisotropy observables:
  - Jet shapes in the $\phi-\eta$ plane. [P. Romatschke and M. Strickland, hep-ph/0309093; P. Romatschke, hep-ph/0607327]
  - Rapidity dependence of medium photons. [B. Schenke and M. Strickland, hep-ph/0606160 and forthcoming]
- A recent paper has shown that including all relevant perturbative effects that the Kolmogorov scaling of a nonabelian ultraviolent avalanche is k^{-1} which for a classical system is thermal. [A.H. Mueller, A.I. Shoshi and S.M.H. Wong, hep-ph/0607136]

Conclusions

- Anisotropic plasmas are qualitatively different than isotropic ones. An entirely new phenomena associated with unstable modes appears.
- For relatively weak anisotropies real-time lattice simulations indicate that for non-abelian plasmas the soft unstable modes “saturate” and the growth then becomes power-law rather than exponential accompanied by cascade/avalance to UV.
- However, for larger anisotropies it appears that exponential field growth can continue similar to an abelian plasma.
- IMPORTANT: Late time soft fields generated by non-abelian instability are isotropic.
- Going beyond the hard-loop approximation by numerically solving the Wong-Yang-Mills equations (CPIC) also shows rapid field growth and an “ultraviolet avalanche”. Results suggest a kind of isotropization “pump”.

Backup #1 – The “ridge”

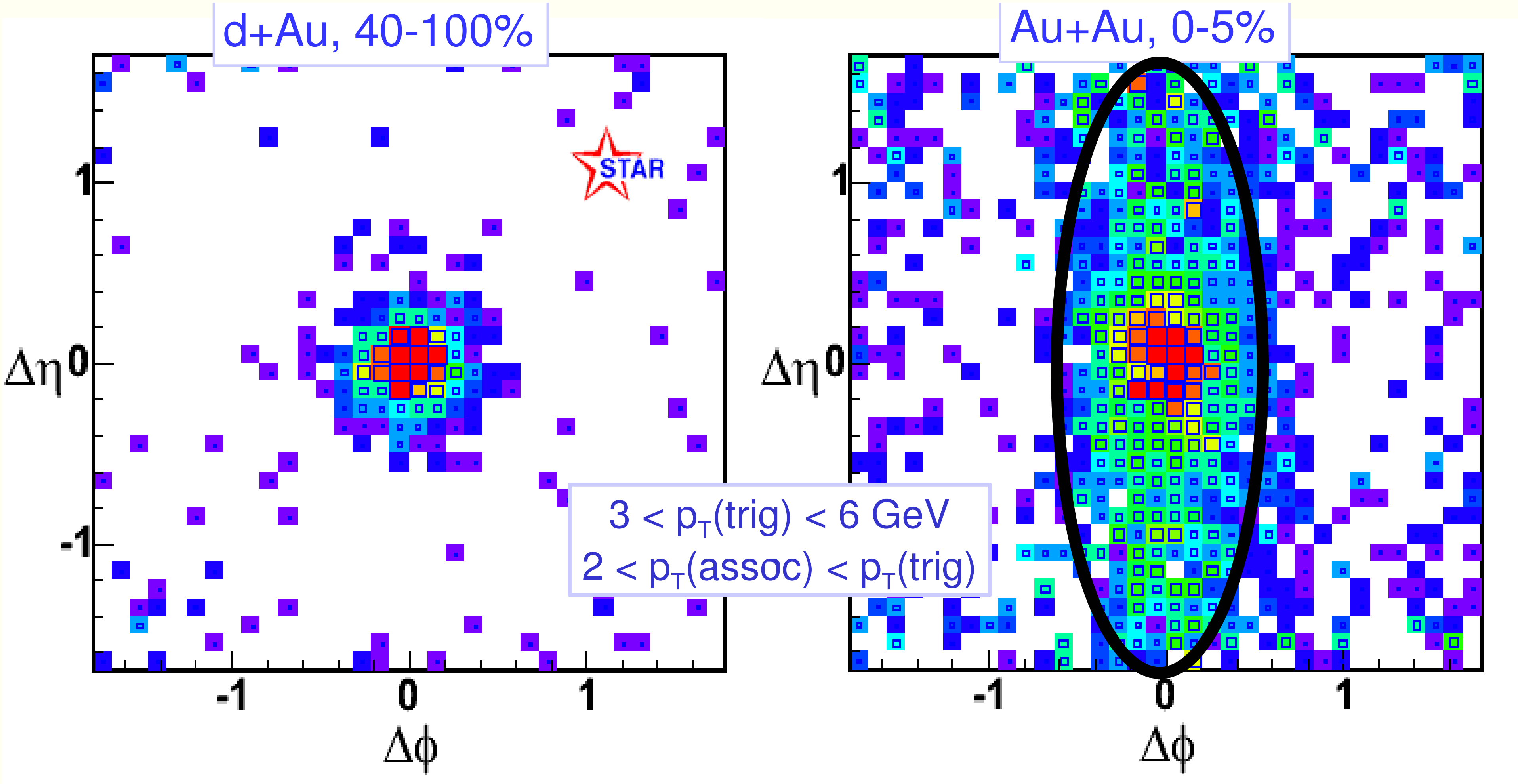

Backup #2 – A note on time scales

- This picture strictly only holds at leading order in $\alpha_s = g^2/4\pi$.
- Instability time scale: $t_{\text{instability}} \sim m_{D,\text{iso}}^{-1} \sim (\sqrt{\alpha}_s Q_s)^{-1}$
- Collisional time scale: $t_{\text{hard collisions}} \sim \left(\alpha_s^2 Q_s\right)^{-1}$

α_s	$t_{\text{collisions}}/t_{\text{instability}}$
0.01	1000
0.1	30
0.3	6

- Can include collisions in the Boltzmann-Vlasov equation and it has been shown that for $\xi \gtrsim 1$ the instabilities persist even for $\alpha_s \sim 0.2 - 0.4$. [B. Schenke, C. Greiner, and M. Thoma, and MS, hep-ph/0603029]

Backup #3 – Pretty picture